creative commons
COMMONS DEED

저작자표시-비영리 2.0 대한민국

이용자는 아래의 조건을 따르는 경우에 한하여 자유롭게

- 이 저작물을 복제, 배포, 전송, 전시, 공연 및 방송할 수 있습니다.
- 이차적 저작물을 작성할 수 있습니다.

다음과 같은 조건을 따라야 합니다:

저작자표시. 귀하는 원저작자를 표시하여야 합니다.

비영리. 귀하는 이 저작물을 영리 목적으로 이용할 수 없습니다.

- 귀하는, 이 저작물의 재이용이나 배포의 경우, 이 저작물에 적용된 이용허락조건을 명확하게 나타내어야 합니다.
- 저작권자로부터 별도의 허가를 받으면 이러한 조건들은 적용되지 않습니다.

저작권법에 따른 이용자의 권리는 위의 내용에 의하여 영향을 받지 않습니다.

이것은 이용허락규약(Legal Code)을 이해하기 쉽게 요약한 것입니다.

Disclaimer

dCollection

공학석사학위논문

형상기억합금 기반의 변형가능한 어그제틱 플라즈모닉 메타물질

Shape memory alloy-based deformable auxetic plasmonic metamaterials

2020 년 8 월

서울대학교 대학원

기계공학부

임 종 혁

Abstract

Shape memory alloy-based deformable auxetic plasmonic metamaterials

Jong-Hyuk Im

Department of Mechanical Engineering

The Graduate School

Seoul National University

Surface plasmon resonance of metallic nanostructures has attracted steady attention for their distinct electromagnetic properties. In particular, localized surface plasmon resonance (LSPR) occurs when light enters conductive nanostructures or nanoparticles smaller than the incident wavelength has been applied to wave absorbers, color filters, and sensors. This is because the resonant frequency can be determined depending on the size, geometry, and dielectric environment of the structures. However, the plasmonic materials developed in the previous researches have a limitation that the resonant frequency could not be changed continuously due to their stationary structure. This problem makes it difficult for practical applications.

In this research, we develop plasmonic metamaterials with auxetic nano patterns that can shift the resonant frequency in the visible region. Shape memory alloy (SMA) wire with 25 μm diameter is used to stretch the patterns and bring them back. Using focused ion beam (FIB), 1 μm thick SMA thin film is fabricated from wire, and the auxetic nano patterns showing remarkable mechanical property are engraved on the film. Gold and silver nanoparticles are sputtered onto the patterned thin film using an ion coater sputtering and e-beam evaporation. We use a micro-gripper to stretch the patterns, and patterns are returned to its original shape by 355 nm laser. To confirm the effect of changing the size of patterns, we not only measure the absorption peak through the spectrometer but also observe the color directly through the microscope. Besides, the finite difference time domain (FDTD) method is used to calculate the reflectance and compare with the experimental results.

Through the above experiment, it is confirmed that various colors appeared depending on the size of auxetic patterns. Also, when the pattern is pulled to increase the size to about 10%, it is measured that the absorption peak moved and the reflection color changed. By returning to the original pattern size using the shape memory effect, deformable auxetic plasmonic metamaterials are demonstrated.

Keywords: Localized surface plasmon resonance, Shape memory alloy, Auxetic, Metamaterials, Plasmonic

Student Number: 2018-26302

Table of Contents

List of Figures

List of Tables

Chapter 1. Introduction

In general, most materials are known to have unalterable intrinsic properties such as chemical, mechanical and optical characteristics. However, when the bulky materials are divided into several nanometers to hundreds of nanometers in size, it exhibits different characteristics from the mass material. This is related to the intermolecular orbit, because the smaller the particle, the more irregular the electron orbit, resulting in a discontinuous energy level - a bandgap. Optically, this bandgap absorbs, scatters, and diffracts light through interaction, allowing control the wavelength of reflection and transmission. As this unique property of nanostructures has been discovered, and as micro-processes have been developed, research on the nanostructures have been conducted in various fields for use as structural color, wavelength absorber, optical sensor, metamaterials, etc.

There are many principles in which nanostructures generate their unique optical properties. Quantum dots, which have been actively researched recently, use photo-luminescence and electro-luminescence. The wavelength range of emission varies depending on the size of the quantum dot. [1] Another major factor is surface plasmon resonance. The plasmons on the metal surface strongly increase absorption and scattering by interacting with the specific energy of the incident light. This effect causes a subtractive color. [2] Diffraction grating has a periodic structure, which splits incident light spatially and diffracts in different directions to generate a color. [3] The thin film multi-layer method selectively absorbs light from a specific wavelength region by using interference. [4] As such, various methods of altering the spectrum of light have been studied.

Among them, metamaterials based on localized surface plasmon resonance (LSPR) which occurs when light enters conductive nanostructures or nanoparticles smaller than the incident wavelength have a great advantage. This is because the

profile of reflected light can be adjusted simply by altering the size, shape, and material of the nanostructure. Besides, resonance occurs at the same wavelength regardless of the angle of the incident light. For these reasons, researches on the optical properties of LSPR has been steadily conducted. [5-7]

However, the LSPR-based metamaterials developed so far have been not tunable in that they use a fixed nanostructure. So, the spectrum could not be continuously adjusted. These lead to the difficulty of producing structures of various shapes and sizes to obtain diverse spectrums.

Here, we develop plasmonic metamaterials that can continuously control the resonance frequency in the visible light region through mechanical actuation. Shape memory alloy (SMA) is used to deform the pattern and restore the original shape by the shape memory effect (SME). The auxetic structure used for patterning has excellent mechanical properties and unique electromagnetic properties. [8] This auxetic structure is based on the re-entrant honeycomb design and has a negative Poisson's ratio, which simultaneously increases the length in the vertical direction during horizontal tension. This increases the size of the overall pattern and makes the absorption peak move clearly. Patterning is performed by using focused ion beam (FIB), and the LSPR effect was enhanced as much as possible by sputtering gold and silver particles. The reflectance before and after the tension is measured using a spectrometer, and also analyzed and compared using a finite-difference time-domain (FDTD) method. Finally, materials that actively shift the absorption peak based on SMA is explored.

Chapter 2. Background

Nanostructures have unique optical properties that do not occur in bulk materials, such as scattering, propagating, absorbing, diffracting or mix of them through interactions with light. LSPR uses scattering and absorbing among them. This chapter provides the principle of LSPR that control the spectrum of light from visible light to infrared. We also examine the pros and cons of this principle and briefly look at the progress of the studies so far. Finally, we find out how these principles work in a complex way and also present the industrial applications of each principle.

2.1. Localized surface plasmon resonance

Surface plasmon resonance (SPR) is a phenomenon in which conductive electrons on a metal surface and external light resonate under certain conditions. Usually, SPR occurs at a specific angle of incident light and greatly increases the absorptance of the metal surface. It is often used as a biosensor to identify the composition of the materials adsorbed on the substrates. [9]

By the way, when the metal nanoparticles or nanostructures smaller than the wavelength of the incident light collide with the phonon, electromagnetic properties are enhanced locally. At this time, the absorption peak shifts according to the size and shape of nanoparticles, nanostructures, not angles, which is called localized surface plasmon resonance. In particular, silver and gold nanoparticles greatly increase this effect. [10,11].

2.2. Applications of localized surface plasmon resonance

LSPR-based nanostructures do not change the resonance energy by the angle of the incident light, which is a representative advantage of LSPR. The area that can maximize this property is coloration. The use of LSPR in the visible light region can produce subtractive colors by absorption of light, which is notable in the field of coloration because it can minimize the color change according to the viewing angle. In fact, this method has been used since ancient Roman times. The evidence is the Lycurgus Cup, a Roman work of art exhibited at the British Museum. (Figure 1) Another example is a stained-glass window representing the Gothic cathedral in the Middle Ages. (Figure 2) The stained glass uses different resonant energy depending on the size of the gold and silver nanoparticles. Figure 2 shows where the colors for gold and silver particles of less than 100 nm are used respectively.

A wave absorber is a practical application in which the most basic characteristics of controlling the electromagnetic wave of LSPR are used. Landy *et al.* developed a perfect wave absorber with an absorptivity of up to 99% using the three-layer called metal-insulator-metal (MIM) structure. (Figure 3)

Application to selective thermal emitters has also been attempted, based on Kirchhoff's thermal radiation law that emissivity and absorptivity of materials are the same. (Figure 4) In this paper, through the microstrip patch array, it was possible to observe the strong heat emission of the same type as the light absorption by SPR at a specific wavelength. In addition, researches have been conducted for use as a detector or sensor using the feature that the operating wavelength can be controlled using the size or shape of the nanostructure. [12, 13]

However, the color using LSPR has low vibrancy. Also, there is a limitation that only metal must be used for the plasmon resonance characteristics, so it is onerousness to produce another structure to control the absorption wavelength band.

Figure 1. The Lycurgus Cup [14]

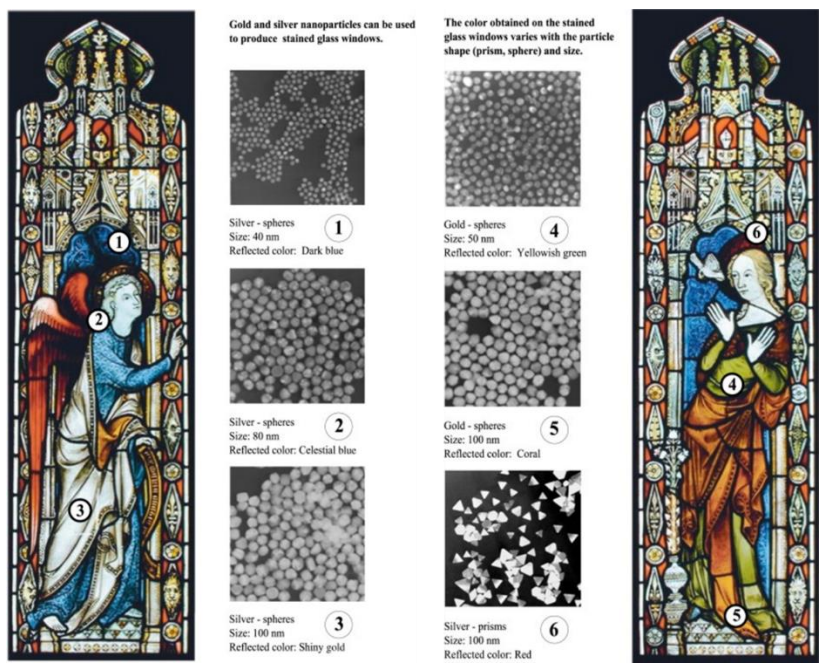

Figure 2. Effect of nanoparticles on the colors of the stained glass windows [15]

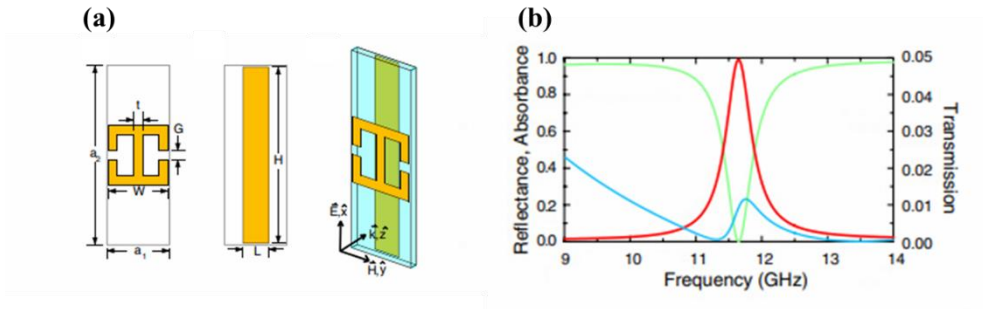

Figure 3. The first developed metamaterial perfect absorber. (a) top layer view, cut wire view, and a perspective view. (b) simulated R(ω) (green), A(ω) (red), T(ω) (blue) [16]

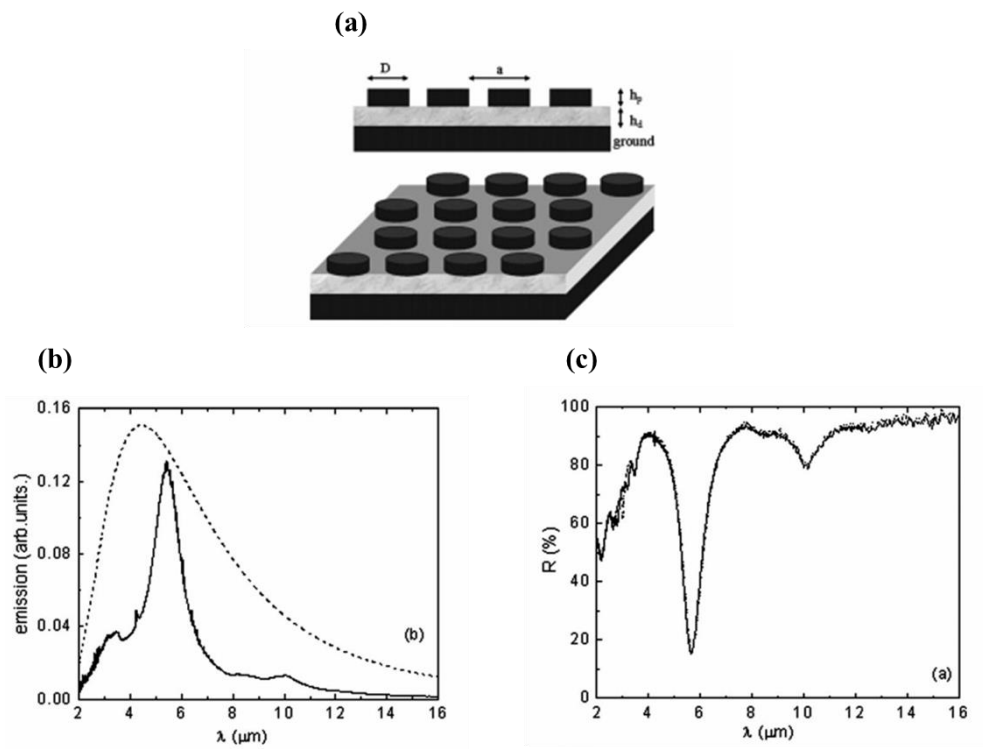

Figure 4. The first developed metamaterial thermal emitter. (a) hexagonal array of circular patches (b) emission (c) reflectivity [17]

2.3. Comparison with other principles

In nano optics, there are various principles that generate unique optical properties. It is necessary to identify each feature to fit the ability required in various fields, and it is shown in Figure 5. The absorber based on the localized surface plasmon resonance uses metal nanoparticles or nanostructures of several nanometers to hundreds of nanometers, so it has good spatial resolution and angle independency but has a poor full width at half maximum (FWHM) characteristics of the absorption spectrum, so the clarity of absorption peak is relatively inferior. Thin film interference-based materials use absorption characteristics in the spectral band as well, but the peak intensity is clear, so the vibrancy of the color is good. However, the reflection spectrum is not constant according to the viewing angle. Diffraction pattern, nanohole array, and other photonic structure reflect only a specific wavelength region, and as with thin film interference, clarity of color is good but it depends on angle.

In fact, these working principles are mostly not used alone. Researchers use a mixture of properties to compensate for the shortcomings of each property, the most important of which is the plasmon on the metal surface. A plasmon is the collective oscillations of free conduction electrons in metals that interact with the specific energy of the incident light according to the surface structure in the dielectric environment. Through interaction, the surface of the metal is electrically polarized to induce a strongly amplified electromagnetic field, and it greatly increases absorption and scattering. One of the most active areas of surface plasmon research is coloration. Various research has been carried out on plasmonic structural color which uses the subwavelength scale effect using EBL and FIB to engrave periodic patterns on the metal film. [18-21] The plasmonic effect is also used in a multi-layer structure by making patterns on the top layer. As such, the surface plasmon has been studied by overlapping with other principles besides itself due to the effect of amplifying the electromagnetic field. (Table 1)

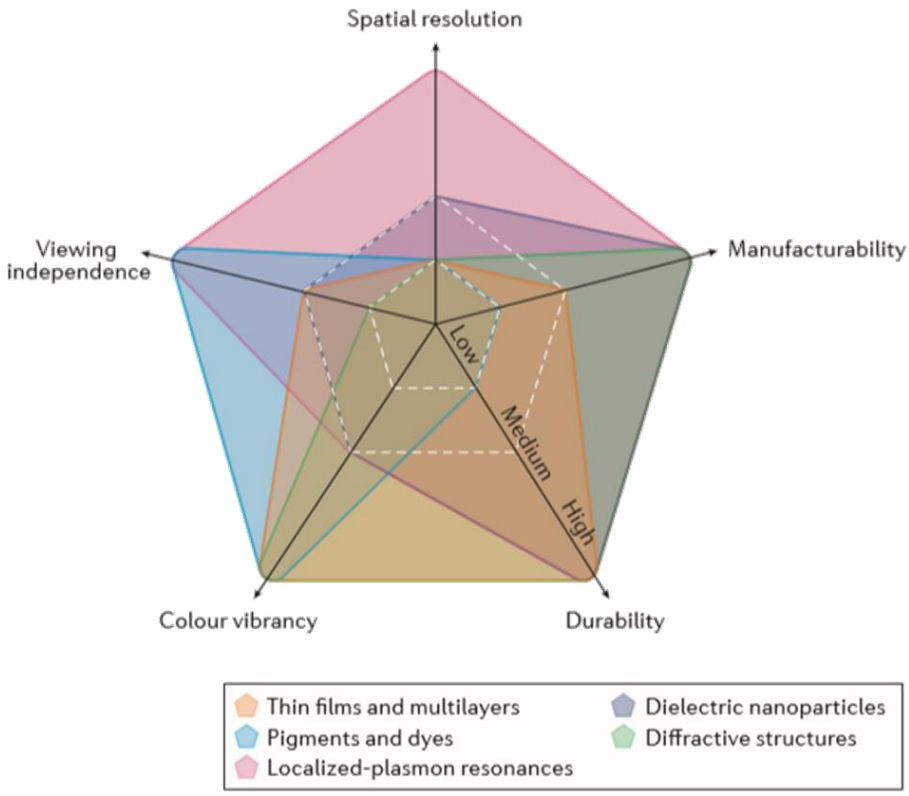

Figure 5. Performance indicators of various nanostructures [22]

Table 1. Types of plasmonic color filter

Diffraction grating	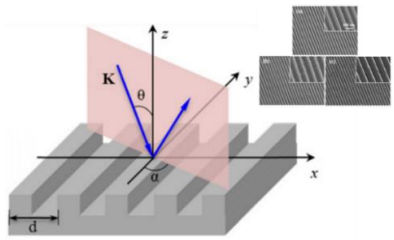 [18]	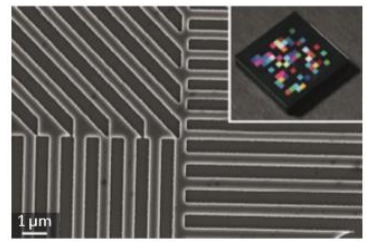 [23]
Nanohole array	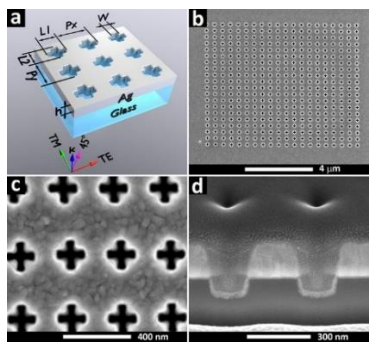 [19]	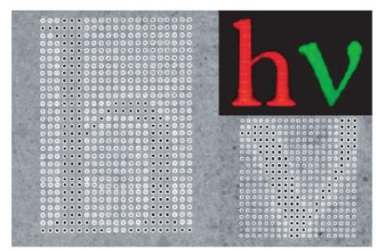 [20]
Multi-layer	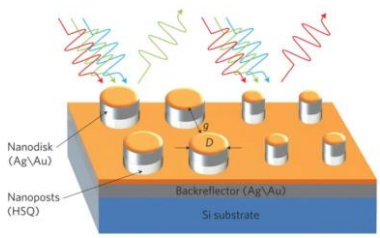 [21]	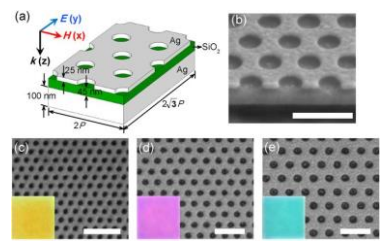 [24]

Chapter 3. Design, fabrication process, experimental setup

This chapter introduces the design, fabrication process, and experimental setup. Shape memory alloy was used for the deformability of the patterns and its type is Nickel-Titanium alloy (nitinol) wire. A nitinol thin film was fabricated using FIB and an auxetic structure called Re-entrant honeycomb was engraved on the thin film. This auxetic structure has a negative Poisson's ratio, and we aimed at a value of -1 to maximize the perpendicular direction of the tensile, leading to a dramatic change in the size of the structure. The thickness of the pattern was determined by considering nitinol's machinability and stability of deformation. After pattern processing, gold and silver thin films were deposited via ion sputtering coater and e-beam evaporation equipment to enhance the LSPR-based absorption effect in the visible region. Through a system comprised of the LED light source, VIS spectrometer, and the optical microscope, the reflectance of the fabricated material was measured in the range of 420 nm to 680 nm and subtractive colors were confirmed. Micro tweezer was used to tension the patterns and a laser with UV wavelength was used for shape memory effect. Section 3.1 introduces the design of the patterns, then the fabrication process and experimental setup are described in sections 3.2 and 3.3, respectively.

3.1. Design of auxetic pattern

The design of the patterns was inspired by the shape of the re-entrant honeycomb. (Figure 6) This form, commonly called the auxetic structure, has been studied in many ways because it has a negative Poisson ratio that is not visible naturally. Geometrically, researches on axial stiffness and bending behavior of auxetic structure demonstrated excellent indentation and buckling resistance of auxetic structure that enables stable tension. [25,26] In addition, this structure is shown to have unique characteristics electronically that have an effective permittivity, which is biaxially anisotropic. [8]

Although the excellent mechanical properties of the auxetic structure had been revealed as described above, we wanted to identify the actual tensile properties of nitinol, not mathematical calculations. A microscale auxetic actuator was manufactured using nitinol wire as shown in Figure 7 (a), and its performance was evaluated in comparison with the previous studies. [27] The tensile force according to the strain was measured via a micro force sensor, and the tensile length was sequentially increased. As a result, it was confirmed that stable tension is possible at a lower stress than the existing diamond-type actuator. (Figure 7. (b))

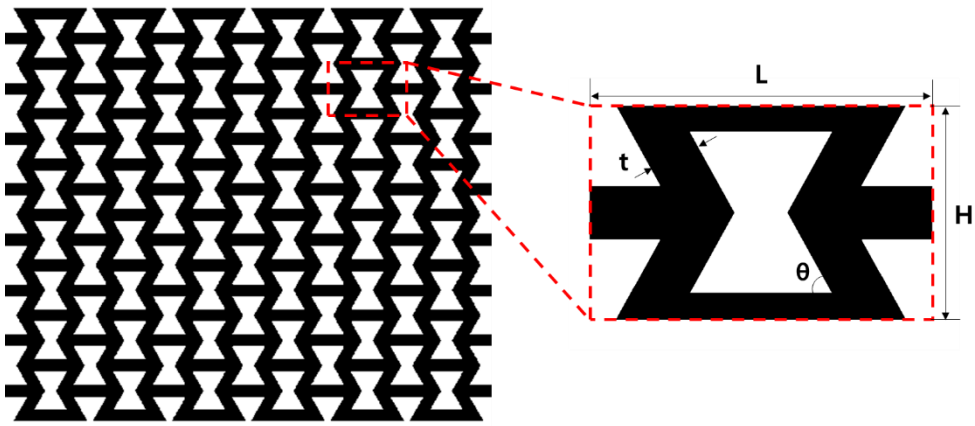

Figure 6. Re-entrant honeycomb auxetic structure

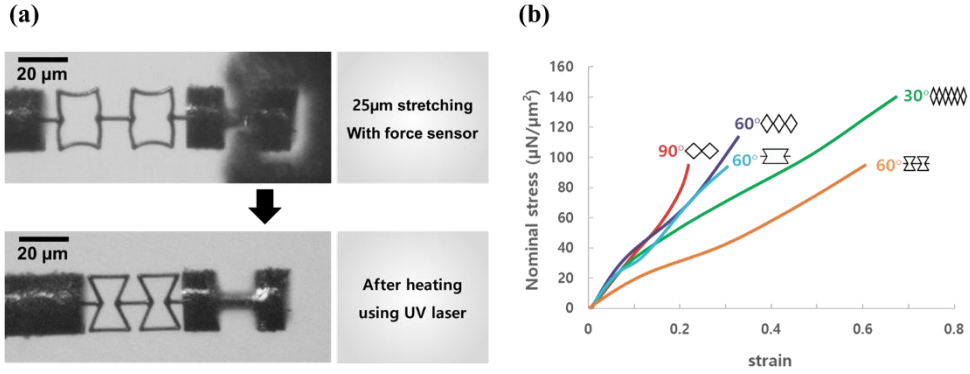

Figure 7. (a) SMA-based micro scale auxetic actuator (b) stress -strain curve of SMA-based micro actuator [27]

Another feature of the auxetic structure is that it has a negative Poisson's ratio. That is, the pattern deformation can be maximized by increasing not only the direction in which the patterns are pulled but also the vertical direction. This property is suitable for this experiment because the absorption peak shifts depending on the size of the deformed pattern. According to previous research, the Poisson's ratio of the auxetic structure depends on the height (H), length (L), and internal angle (θ) shown in Figure 6. [28] The results of the research are shown in Figure 8. Based on this table, the size of the H/L and the internal angle were determined so that the Poisson's ratio would be -1. Figure 9 is nano patterns actually fabricated, and surface plasmon resonance occurs in the infrared region and visible region respectively.

	H/L		1.5	2	2.5	3	3.5	4
λ	$\pi/18$	ν_X	−4.211	−3.058	−2.40	−1.976	−1.679	−1.460
	$\pi/9$		−2.230	−1.557	−1.196	−0.971	−0.818	−0.706
	$\pi/6$		−1.5	−1	−0.75	−0.6	−0.5	−0.429
	$2\pi/9$		−1.065	−0.673	−0.492	−0.387	−0.320	−0.272
	$5\pi/18$		(−0.735)	−0.437	−0.311	−0.241	−0.197	−0.167
	$\pi/3$		(−0.455)	−0.255	−0.177	−0.135	−0.110	−0.092

Figure 8. Poisson's ratio of auxetic structure at small deformation [28]

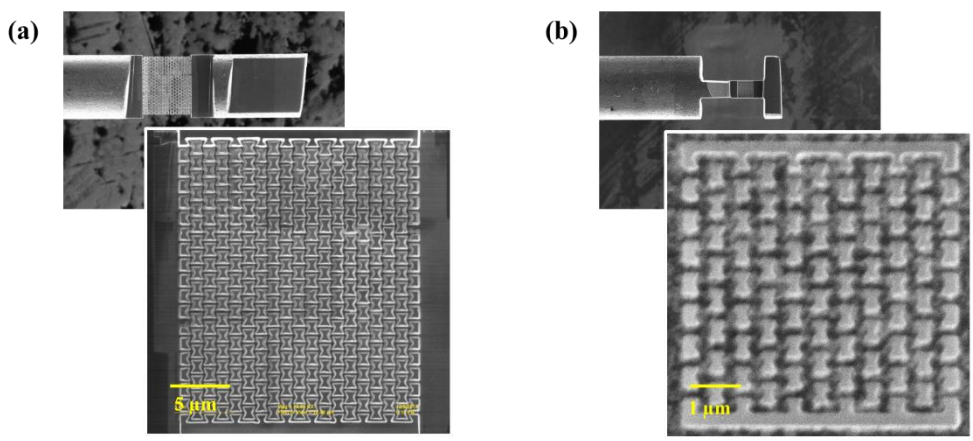

Figure 9. SED image of auxetic structure (a) infrared region (b) visible region

3.2. Fabrication process

The process of cutting and patting nitinol via FIB was developed. The nitinol used in this experiment is a shape memory alloy composed of 50% nickel and titanium, and phase transformation occurs at 70 °C, making it relatively resistant to heat. (Dynalloy, Inc., Costa Mesa, CA, USA) The detailed characteristics are in Table 2, and the SMA phase transition process is illustrated in Figure 10. This nitinol is a smart material that reacts to heat reversibly and has high biocompatibility, thus giving the possibility of being used in a diversity of fields. [29]

Table 2. Nitinol physical properties

Density		**6.45 g/cm^3**
Specific Heat		**0.2 cal/g × °C**
Melting Point		**1300 °C**
Latent Heat of Transformation		**5.78 cal/g**
Thermal Conductivity		**0.18 W/cm × °C**
Transition Temperature		**70 °C**
Poisson Ratio		**0.33**
Thermal Expansion Coefficient	**Martensite**	**6.6×10^{-6} /°C**
	Austenite	**11.0×10^{-6}/°C**
Electrical Resistivity	**Martensite**	**80 micro-ohms × cm**
	Austenite	**100 micro-ohms × cm**

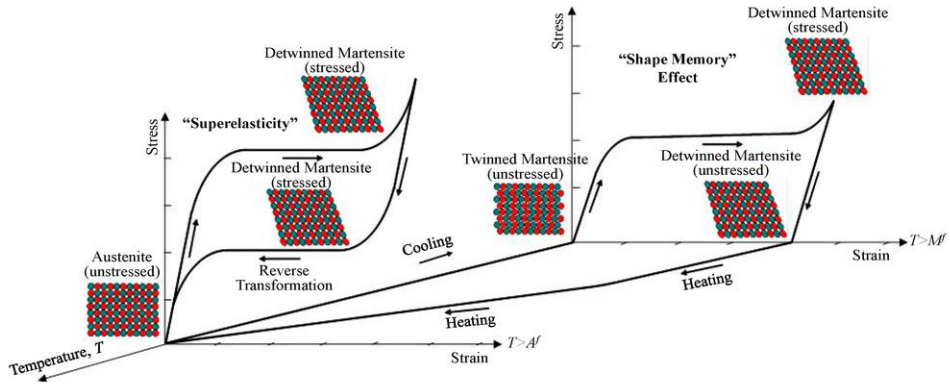

Figure 10. Phase transition of shape memory alloy [30]

Figure 11 shows the overall process for fabricating SMA-based plasmonic metamaterials. The first step is to cut SMA thinly via FIB to produce about 1 μm thickness of the film. Subsequently, the patterning was also performed with FIB after rotating the specimen by 90 degrees. At this time, the patterns were carved with an interval of about 15 nm to identify the change of absorption peak according to the size of the auxetic structure and to see the subtractive color. Later, gold and silver nano film were deposited via ion sputtering coater and e-beam evaporation equipment. This is because the FDTD analysis demonstrated that thickness of more than 50 nm is not very helpful in improving reflectivity. (Figure 12)

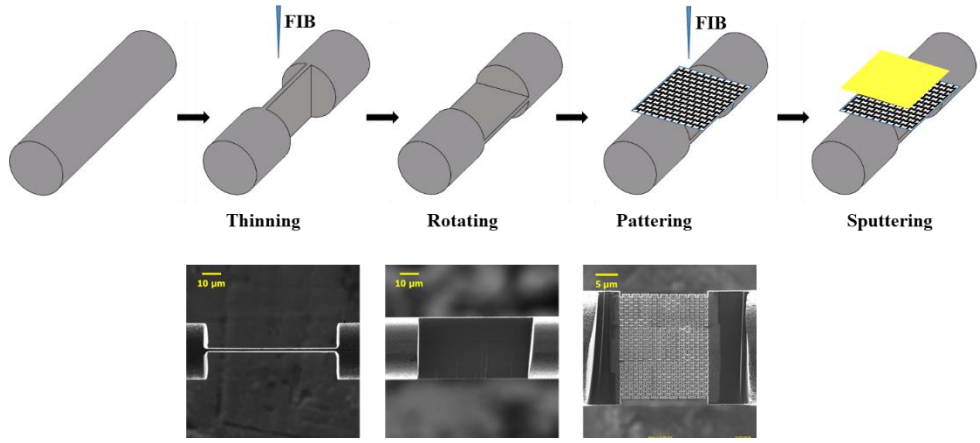

Figure 11. Fabrication process of SMA-based plasmonic metamaterials

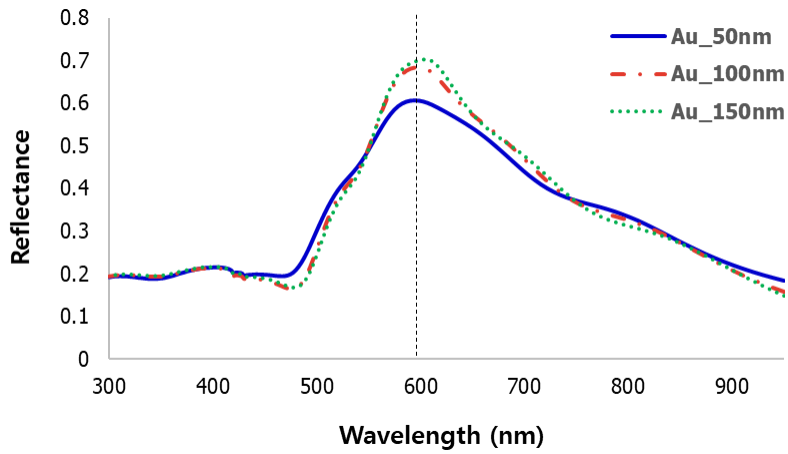

Figure 12. Reflectance of auxetic plasmonic materials with gold film thickness via FDTD method

3.3. Experimental setup

This section introduces an experimental setup dealing with plasmonic metamaterials. The overall form is shown in Figure 13. An upright microscope (BX53MTRF-S, Olympus, Tokyo, Japan) was used to observe the reflected image. A spectrometer (FLAME-S-UV-VIS, Ocean Optics, Largo, USA) was coupled to a microscope to measure the spectrum reflected when LED light was incident. The manual controller and Automatic controller were used for the operation of the 3-axis nano stage. In order to confirm the change in the absorptance during tension, the metamaterial sample for measurement and a microgripper were respectively coupled to two 3-axis nano stages, and detailed form is shown in Figure 14. Finally, a control platform was constructed that can simultaneously measure spectral data while observing the images through a microscope.

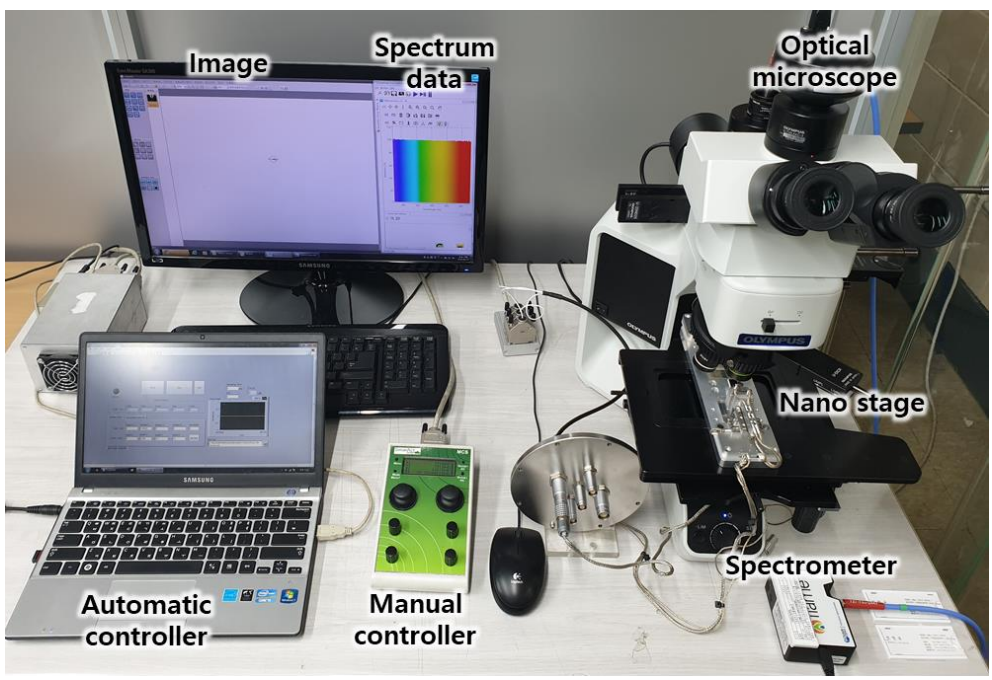

Figure 13. Experimental setup for spectrum measurement

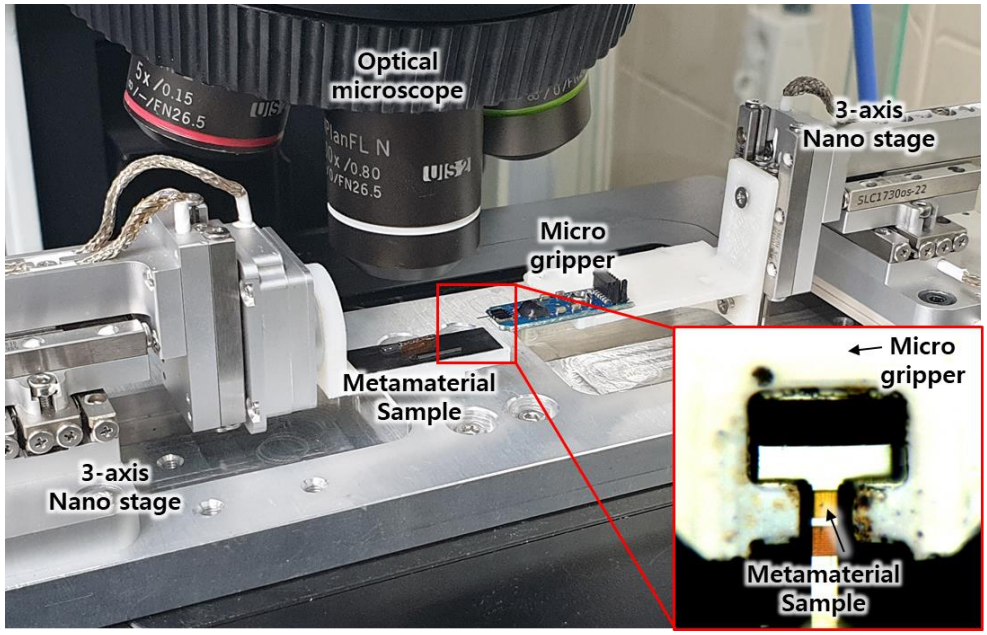

Figure 14. Control platform for tensile test

Chapter 4. Localized surface plasmon resonance depending on the auxetic pattern size

In this chapter, we introduce the change in absorption wavelength according to the auxetic pattern size of developed metamaterials. The size of the auxetic patterns was determined to cause localized surface plasmon resonance in the visible wavelength region. Also, the overall shape of auxetic patterns was maintained although the size was changed.

First, in order to confirm the position of the absorption peak according to the size of the patterns, several patterns with specific intervals were produced. Then, we sputtered silver and gold film on the fabricated patterns. In this process, we also confirmed the excellent LSPR effect of silver and gold film by comparing before and after the deposition of these metal films. Lastly, in each case, the reflective color was observed through an optical microscope, and the experimental results were verified by comparing the measured spectral data and the simulated data from FDTD.

4.1. The influence of Ag film in LSPR

The shape memory effect of nitinol is differentiated from other metals, enabling tension and recovery of patterns. However, as explained in the previous chapter, nitinol is known to have a relatively weak LSPR effect in the visible region compared to silver and gold. This section demonstrated that difference by comparing the reflection spectrum of patterns made only with nitinol and patterns deposited with silver.

The picture to the right of Figure 15 shows the metamaterials that were fabricated. For the tension of the pattern, the shape of the entire sample was made to match the shape of a micro tweezer. A spectrum of vertical reflectance with LED light was measured before and after the deposition of Ag film and observed through an optical microscope. The results are shown in the graph on the left. The graph shows the reflection spectrum for before and after Ag deposition for the top pattern in the photo on the right. In both cases, the positions of the absorption peaks were the same, but as a whole, they were more pronounced after deposition. In addition, this result could be confirmed by the reflection color in the picture on the right. This was the same for Au, and thus, the production of metamaterials was completed by laminating about 50 nm silver and gold thin film through e-beam evaporation and ion coater sputtering respectively.

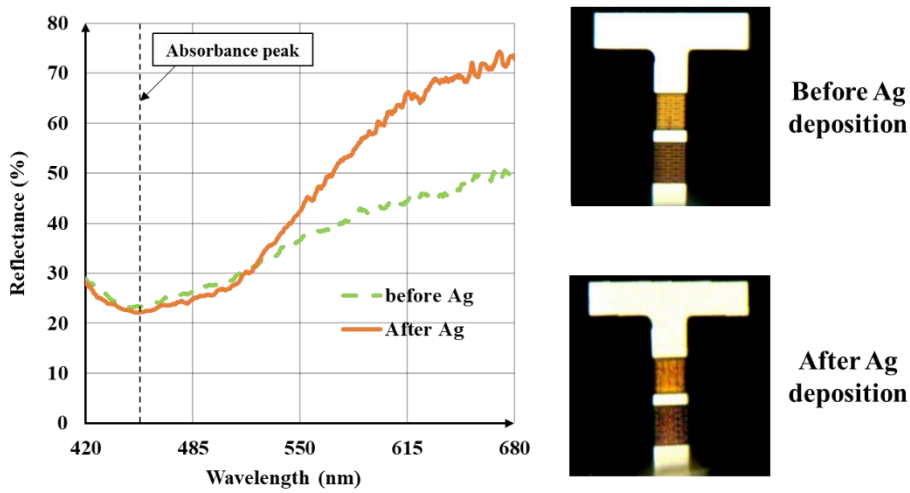

Figure 15. Before and after Ag thin film deposition (a) reflection spectrum (b) image from optical microscope

4.2. Reflectance depending on the pattern size with Ag film

The metamaterials developed in this research are based on LSPR, so the wavelength range in which light absorption occurs varies depending on the size or shape of the patterns. As shown in Figure 16, SMA-based auxetic patterns of different sizes were produced via FIB. After FIB processing, Au and Ag thin films were deposited on the patterns to amplify the absorption effect, as demonstrated in the previous section. First, this section shows the experimental results when Ag thin films were laminated.

The spectrometer measurement results and optical microscopy images of metamaterials with about 50 nm Ag film are shown in Figure 17. Each pattern on the right side of Figure 17 forms a size ranging from 500 nm × 810 nm to 650 nm × 1080 nm based on the height × width of the auxetic pattern shape in Figure 6. The measurement wavelength area is from 430 nm to 680 nm, which is close to the general visible light range, and the plasmon resonance of the patterns that occurred in this area. As a result, maximum light absorption of each pattern occurs at (a) 450 nm, (b) 500 nm, (c) 545 nm, (d) 575 nm, and (e) 610 nm. The overall tendency is that as the size of the pattern increases, the absorption wavelength region also increases, which proves that the localized surface plasmon resonance phenomenon is occurring.

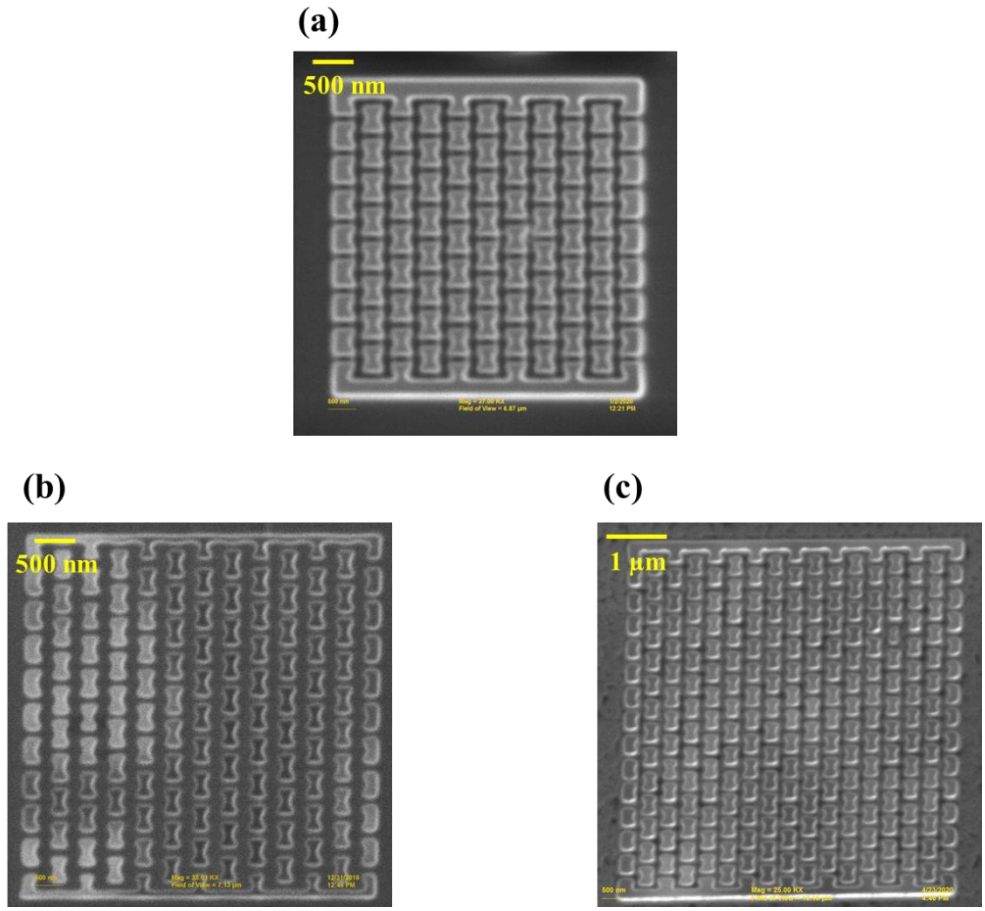

Figure 16. SED image of different sized auxetic patterns
(a) 500 nm × 810 nm, (b) 550 nm × 900 nm, (c) 585 nm × 965 nm

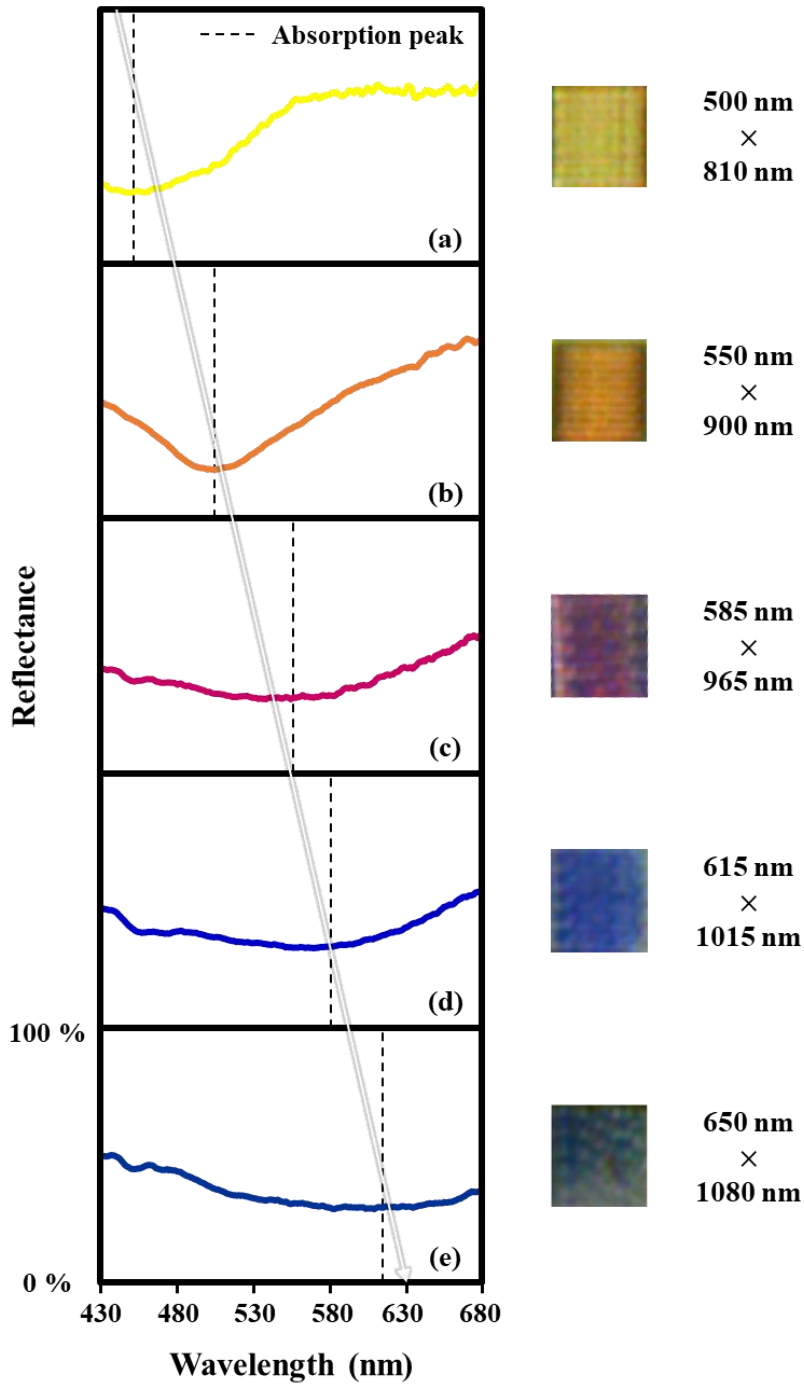

Figure 17. Reflectance and microscopy image under varying the patterning size. The maximum absorption occurs at (a) 450 nm, (b) 500nm, (c) 545 nm, (d) 575 nm (e) 610 nm

To prove the actual experimental results, 3D models of the same shape were depicted to obtain reflectance data for vertical reflection of light through the FDTD method. The modeling is shown in Figure 18. For the silver film, the refractive index of CRC was used, and in the case of nitinol, the refractive index ($\tilde{N} = n - jk$) actually measured using ellipsometry was used. In the analysis area of the FDTD, the boundary condition of the sides was selected as symmetry and anti-symmetry condition so that the same auxetic pattern is periodically replicated infinitely. In addition, perfectly matched layer (PML) boundary was adopted for the top and bottom surfaces so that 100% of the light is absorbed when it touched, so as not to affect within the analysis area. The results are shown in Figure 19. The absorptions were maximum at (a) 455 nm, (b) 510 nm, (c) 545 nm, (d) 565 nm, and (e) 600 nm, respectively. There was only an error up to 10 nm wavelength compared with experimental results. Also, the absorption peak can be clearly observed in the simulation results than the actual experiments.

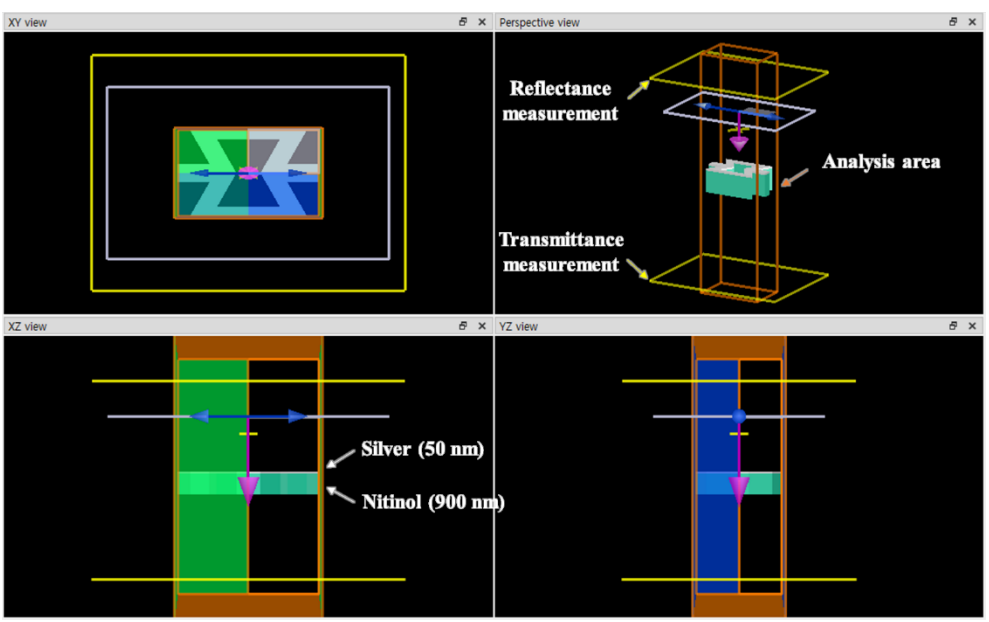

Figure 18. Finite difference time domain image of auxetic metamaterials

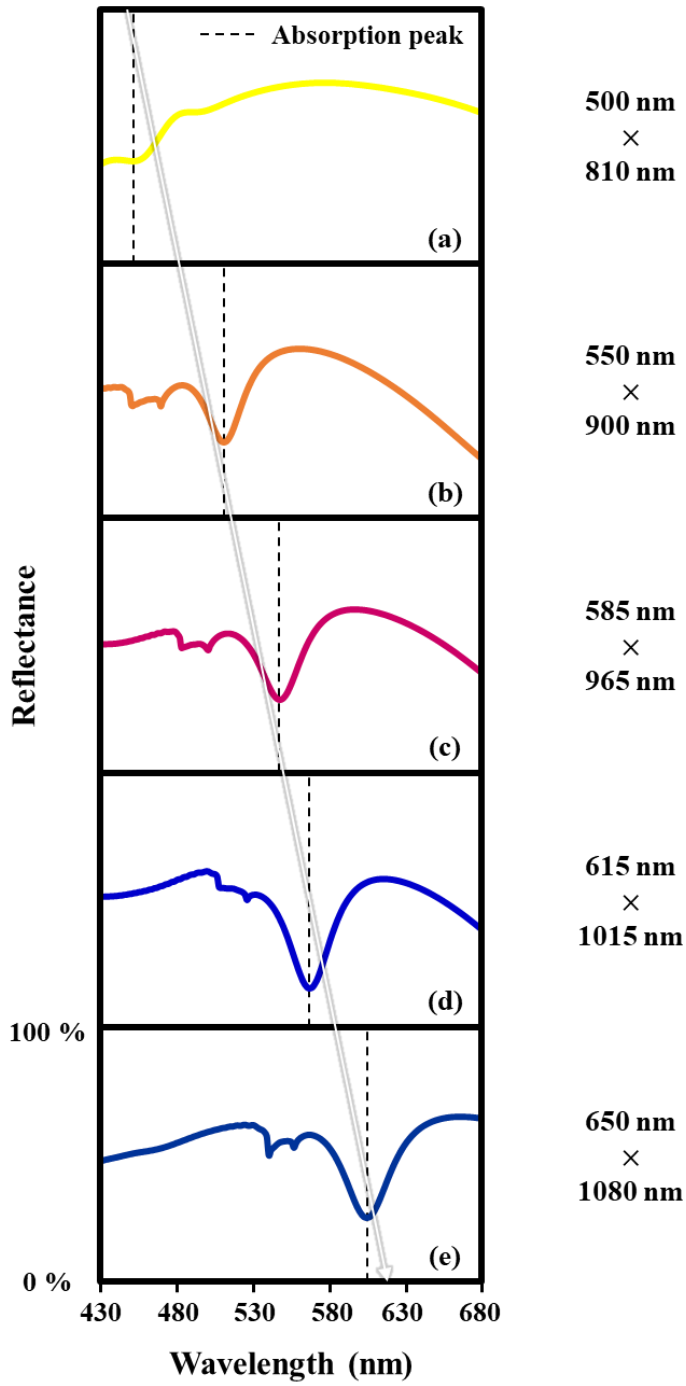

Figure 19. Reflectance via FDTD under varying the patterning size. The maximum absorption occurs at (a) 455 nm, (b) 510nm, (c) 545 nm, (d) 565 nm (e) 600 nm

4.3. Reflectance depending on the pattern size with Au film

Like the silver film, the gold film is also a metal that maximizes the LSPR phenomenon in the visible area. In order to confirm the LSPR effect of gold film, we introduce the change of reflectance according to the size of the pattern when the gold thin film is deposited on metamaterials engraved with auxetic pattern fabricated by using FIB. At this time, the gold film was deposited about 50 nm through an ion sputtering coater.

The actual measured reflection spectrum and color according to the pattern size are shown in Figure 20. For pattern sizes from 500 nm × 810 nm to 650 nm × 1080 nm, as the overall pattern size of the reflectance increases, the position of the absorption peak tends to increase. The positions of the absorption peaks are (a) 445 nm, (b) 530 nm, (c) 570 nm, and (d) 620 nm. However, the gold film, unlike silver, has a very low reflectance in the blue region (~ 485 nm). Therefore, it was difficult to observe the CMY colors, and the colors related to blue were not found. Therefore, in the next chapter's tensile test, a silver film was deposited to confirm the color change using all colors.

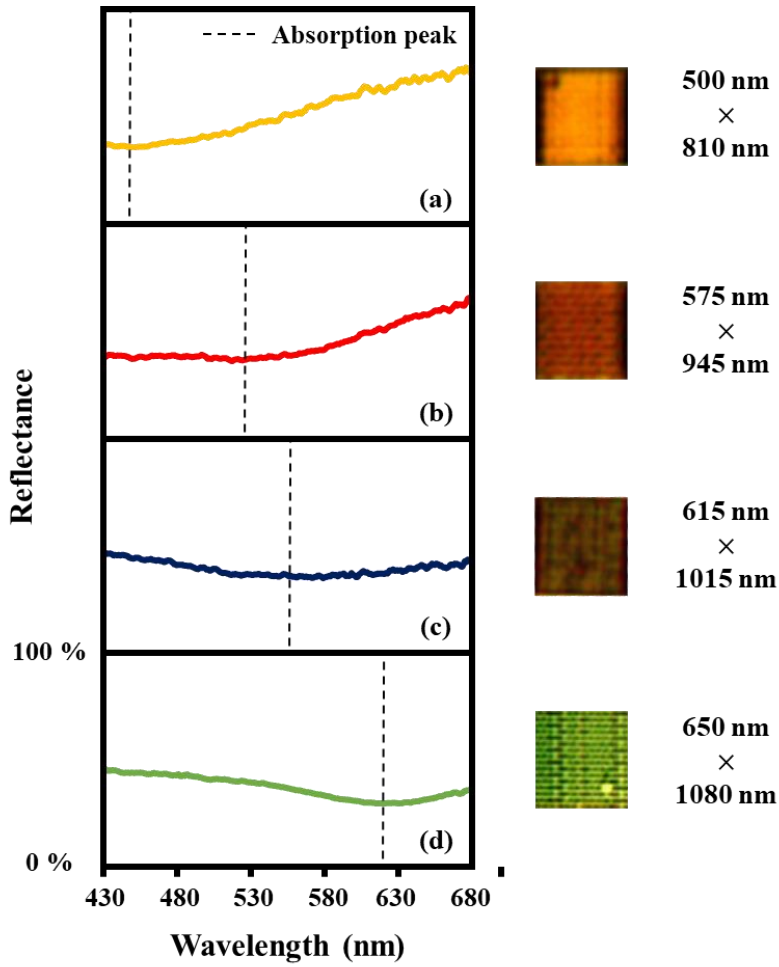

Figure 20. Reflectance and microscopy image under varying the patterning size. The maximum absorption occurs at (a) 445 nm, (b) 530nm, (c) 570 nm, (d) 620 nm

Chapter 5. Localized surface plasmon resonance of pattern under tension loading

This chapter introduces an experiment that stretches the patterns and shifts the wavelength where the LSPR phenomenon occurs as its size increases. As confirmed in the previous section, in the case of gold film, the reflectance is not sufficiently high below the blue wavelength (~ 485 nm), so that the corresponding color and absorption spectrum results cannot be obtained. Therefore, on the pattern tension specimen, about 50 nm silver film was deposited through an e-beam evaporation process.

To stretch the pattern, two 3-axis nano stages were combined with an optical microscope. (Figure 13, Figure 14) Several samples for tension were produced in a T-shape so that it could be pulled with a gripper. (Figure 21)

In general, if the patterns are stretched in one direction, it contracts in a perpendicular direction to it. However, the negative Poisson's ratio of the auxetic patterns used in this experiment complements this so that the patterns can be enlarged in all directions so that the pattern size can be maximized with a small tensile distance. In addition, it has excellent stability in tension. Therefore, it is very suitable for tension.

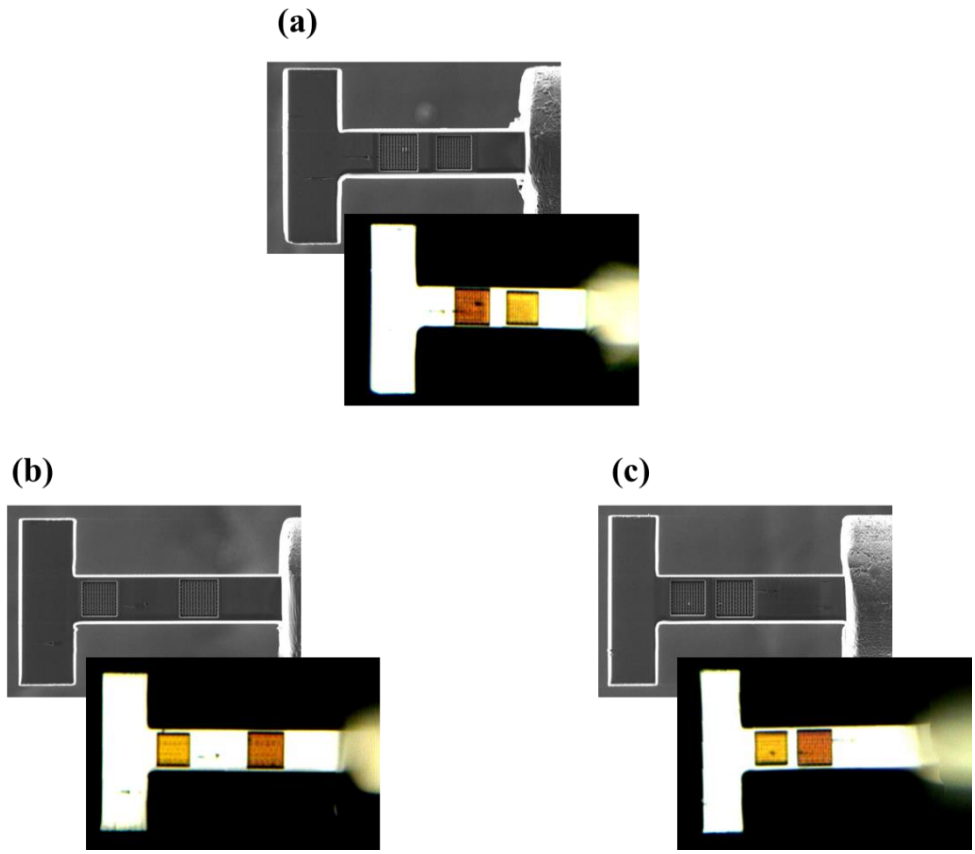

Figure 21. T-shape pattern samples for tension

5.1. Reflectance change of pattern under tension loading

This section shows the spectrum and color change when different size patterns are stretched. Figure 22 shows the results when the metamaterials in Figure 21 were tensioned. Based on the yellow pattern of the sample (pattern size : 500 nm × 810 nm), the maximum absorption occurred at 439 nm wavelength before stretching, but the absorption peak appeared at 500 nm after stretching. This could also be confirmed by optical microscope measurements. The yellowish color gradually changed to orange. In order to prove that the absorption peak is shifted according to the size change, the size change of the auxetic patterns was confirmed through microscopic image analysis. As a result, it was verified that one auxetic pattern was increased by about 55 nm and was similar to the degree of the peak position shift.

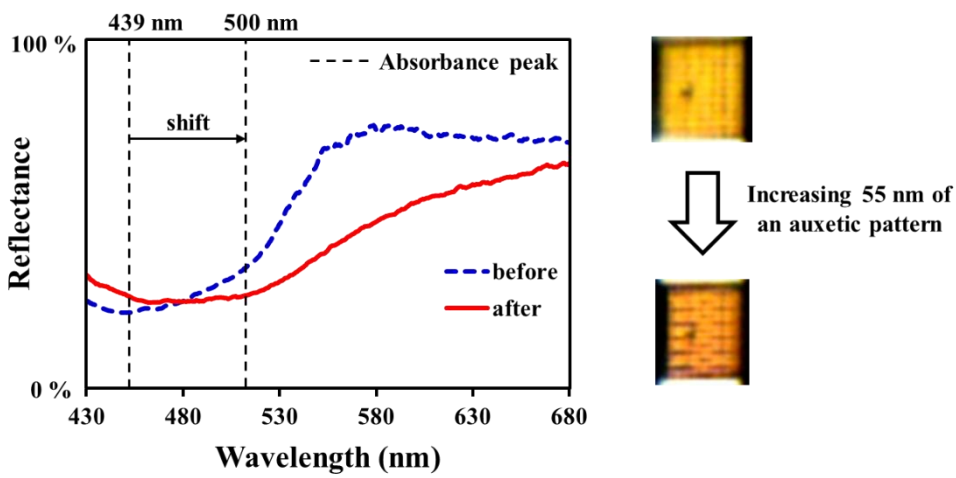

Figure 22. Color and spectrum change of 500 nm × 810 nm pattern under tension loading

Second, the same experiment was conducted for a pattern having a size of 605 nm × 990 nm. The results are shown in Figure 23. The color that showed a slight magenta tendency before tension had a more blue color after the tension. Spectrum measurements confirm this observation. The maximum absorption occurred before and after tensile at 564 nm and 595 nm respectively.

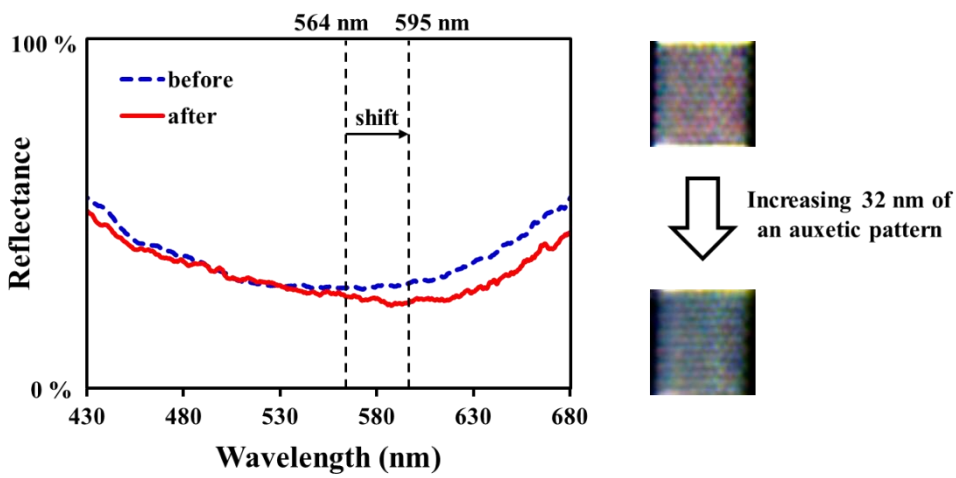

Figure 23. Color and spectrum change of 605 nm × 990 nm pattern under tension loading

The final tensile experiment was conducted in the same method for a pattern having a size of 560 nm × 915 nm. The results are shown in Figure 24. Initially, absorption was highest at 524 nm, but it shifted to 547 nm after stretching. As the overall tensile length was not large, the shift of the spectrum was small, so it was confirmed that the change in the reflected color was not obvious, but the color that was close to red was slightly pale.

Lastly, the pattern was restored to its original size by the shape memory effect, a characteristic of the SMA. As a result, it can be confirmed that the reflection spectrum almost completely returned to the spectrum before the deformation. Since the patterning area is small and the number of patterns is insufficient, the results of color change and spectral measurement are not very clear, but this tensile experiment proved the possibility for deformable plasmonic metamaterials.

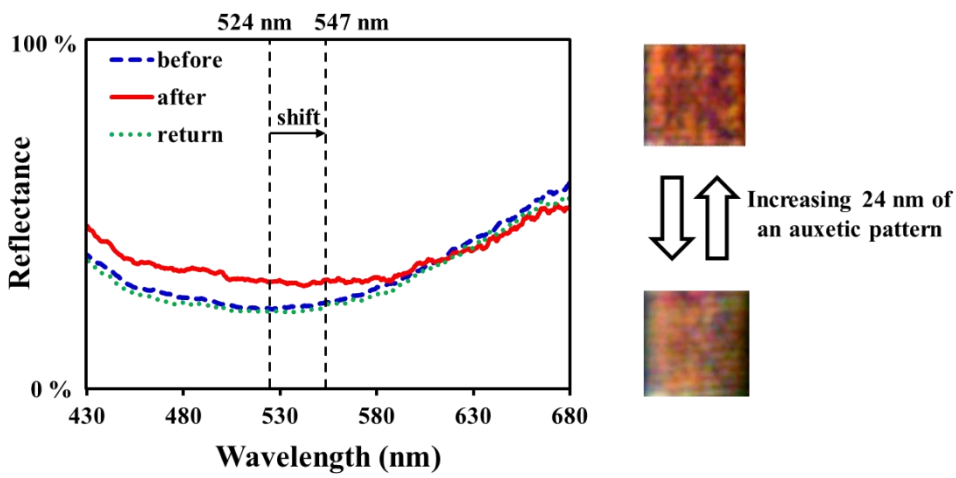

Figure 24. Color and spectrum change of 560 nm × 915 nm pattern under tension loading

5.2. Applications of deformable metamaterials

The plasmonic metamaterials that control the electromagnetic wave have been applied in various fields as explained in section 2.2, and have a huge potential that can be developed in the future. In particular, in this paper, deformable metamaterials using properties of SMA were developed, which not only are applicable to proposed applications but also make tunability. First, this tunability opens up the applicability to light modulators. The existing plasmonic metamaterial-based light modulator controlled light through a complicated pixel configuration and diode biasing method. [31] However, the metamaterials developed here can omit the complicated production process, which is time-consuming and costly, while enabling light control through simple a operation. Another accessible tunable metamaterial application is the color filter. Since our experiments showed that it can operate in the visible spectrum realm, it can be applied in the manner shown in Figure 25 through large-area patterning.

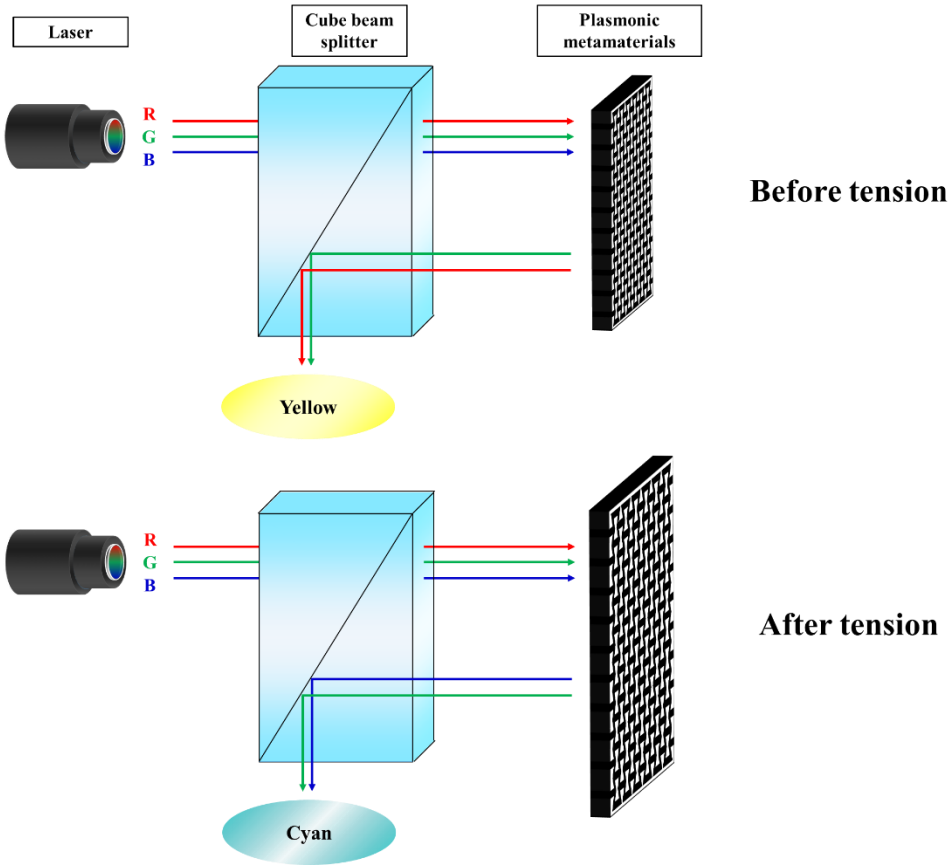

Figure 25. Application as a color filter of tunable auxetic plasmonic metamaterials

Chapter 6. Conclusions

Metamaterials are arrays composed of subwavelength nano elements and control electromagnetic waves based on their unique electric permittivity and magnetic permeability. Since they have special abilities that cannot be commonly found in nature, they have been steadily researched for use in a variety of applications since their inception. Nevertheless, currently developed plasmonic metamaterials have some problems to overcome. First, the manufacturing process is complicated, and the 3D structure cannot be manufactured due to process limitations. Second, most materials cannot be operated at a faster range than the infrared frequency. In addition, the plasmonic metamaterials developed to date have not escaped the stationary shape in that it uses metal. This is a very time-consuming and costly operation because it requires the structures of different sizes and shapes to operate at different wavelengths.

In this research, deformable plasmonic metamaterials were developed to overcome the hurdles encountered by these metamaterials. The LSPR effect was enhanced by coating gold and silver films through physical vapor deposition on auxetic nano patterns based on a shape memory alloy fabricated by using a focused ion beam. First, the reflectance was measured depending on the pattern size. When the gold film was deposited, the colors except for the blue area were confirmed, and when the silver film was deposited, all CMY colors were observed. And the change in reflectance was also confirmed when patterns were pulled. When the size of the pattern changed by up to 10%, the absorption peak shifted as much as it altered, and the reflection color changed from yellow to orange or from magenta to blue. Finally, the patterns were returned to its original size by the shape memory effect. This is the biggest difference from the previous research, so it is possible to control the light actively. Besides, it uses the localized surface plasmon resonance, so it has a

superiority that it is not angle sensitive.

The metamaterials developed in this research can be further improved. Despite the clear color observed by the eye, the actually measured spectrum was not as good as the simulated result. This is because the area of the patterning region is relatively small (7 μm × 7 μm or less) and reflectance is greatly influenced by external light. Also, the pattern thickness was not sufficiently thick, so that the tensile displacement could not be enough long. Nevertheless, since it proved the active movement of the absorption peak, it has great implications for the future aspects of the development of tunable metamaterials.

As discussed in the previous chapters, plasmonic metamaterials are being applied in most fields such as wave absorbers, light modulators, thermal emitters, color filters, biosensors where electromagnetic waves are being used. New relevant theories continue to be uncovered, and the scope of their application is gradually expanding. Although it is still insufficient in terms of cost, time, and stability to be applied as a practical device, metamaterials will overcome difficulties based on its potential to have a great impact on current nanotechnology.

References

[1] Zhang, F., Zhong, H., Chen, C., Wu, X. G., Hu, X., Huang, H., . & Dong, Y. (2015). Brightly luminescent and color-tunable colloidal CH3NH3PbX3 (X= Br, I, Cl) quantum dots: potential alternatives for display technology. *ACS nano*, *9*(4), 4533-4542.

[2] Barnes, W. L., Dereux, A., & Ebbesen, T. W. (2003). Surface plasmon subwavelength optics. *nature*, *424*(6950), 824-830.

[3] Lochbihler, H. (2009). Colored images generated by metallic sub-wavelength gratings. *Optics express*, *17*(14), 12189-12196.

[4] Diest, K., Dionne, J. A., Spain, M., & Atwater, H. A. (2009). Tunable color filters based on metal− insulator− metal resonators. *Nano letters*, *9*(7), 2579-2583.

[5] Jensen, T. R., Malinsky, M. D., Haynes, C. L., & Van Duyne, R. P. (2000). Nanosphere lithography: tunable localized surface plasmon resonance spectra of silver nanoparticles. *The Journal of Physical Chemistry B*, *104*(45), 10549-10556.

[6] Valente, J., Plum, E., Youngs, I. J., & Zheludev, N. I. (2016). Nano-and Micro-Auxetic Plasmonic Materials. *Advanced Materials*, *28*(26), 5176-5180.

[7] Takimoto, B., Nabika, H., & Murakoshi, K. (2009). Enhanced Emission from Photoactivated Silver Clusters Coupled with Localized Surface Plasmon Resonance. *The Journal of Physical Chemistry C*, *113*(27), 11751-11755.

[8] Smith, F. C., Scarpa, F., & Chambers, B. (2000). The electromagnetic properties of re-entrant dielectric honeycombs. *IEEE Microwave and Guided Wave Letters*, *10*(11), 451-453.

[9] Ding, S. Y., Yi, J., Li, J. F., Ren, B., Wu, D. Y., Panneerselvam, R., & Tian, Z. Q. (2016). Nanostructure-based plasmon-enhanced Raman spectroscopy for surface analysis of materials. *Nature Reviews Materials*, *1*(6), 1-16.

[10] Choi, B. H., Lee, H. H., Jin, S., Chun, S., & Kim, S. H. (2007). Characterization of the optical properties of silver nanoparticle films. *Nanotechnology*, *18*(7), 075706.

[11] Amendola, V., Pilot, R., Frasconi, M., Maragò, O. M., & Iatì, M. A. (2017). Surface plasmon resonance in gold nanoparticles: a review. *Journal of Physics: Condensed Matter*, *29*(20), 203002.

[12] Tao, H., Kadlec, E. A., Strikwerda, A. C., Fan, K., Padilla, W. J., Averitt, R. D., ... & Zhang, X. (2011). Microwave and terahertz wave sensing with metamaterials. *Optics express*, *19*(22), 21620-21626.

[13] Liu, N., Mesch, M., Weiss, T., Hentschel, M., & Giessen, H. (2010). Infrared perfect absorber and its application as plasmonic sensor. *Nano letters*, *10*(7), 2342-2348.

[14] Kumar, N., & Kumar, R. (2013). *Nanotechnology and Nanomaterials in the Treatment of Life-threatening Diseases*. William Andrew.

[15] Loos, M. (2014). *Carbon nanotube reinforced composites: CNT Polymer Science and Technology*. Elsevier.

[16] Landy, N. I., Sajuyigbe, S., Mock, J. J., Smith, D. R., & Padilla, W. J. (2008). Perfect metamaterial absorber. *Physical review letters*, *100*(20), 207402.

[17] Puscasu, I., & Schaich, W. L. (2008). Narrow-band, tunable infrared emission from arrays of microstrip patches. *Applied Physics Letters*, *92*(23), 233102.

[18] Seo, M., Lee, J., & Lee, M. (2017). Grating-coupled surface plasmon resonance on bulk stainless steel. *Optics express*, *25*(22), 26939-26949.

[19] Balaur, E., Sadatnajafi, C., Kou, S. S., Lin, J., & Abbey, B. (2016). Continuously tunable, polarization controlled, colour palette produced from nanoscale plasmonic pixels. *Scientific reports*, *6*, 28062.

[20] Genet, C., & Ebbesen, T. W. (2010). Light in tiny holes. In *Nanoscience And Technology: A Collection of Reviews from Nature Journals* (pp. 205-212).

[21] Kumar, K., Duan, H., Hegde, R. S., Koh, S. C., Wei, J. N., & Yang, J. K. (2012). Printing colour at the optical diffraction limit. *Nature nanotechnology*, *7*(9), 557.

[22] Kristensen, A., Yang, J. K., Bozhevolnyi, S. I., Link, S., Nordlander, P., Halas, N. J., & Mortensen, N. A. (2016). Plasmonic colour generation. *Nature Reviews Materials*, *2*(1), 1-14.

[23] Christiansen, A. B., Højlund-Nielsen, E., Clausen, J., Caringal, G. P., Mortensen, N. A., & Kristensen, A. (2013, September). Imprinted and injection-molded nano-structured optical surfaces. In *Nanostructured Thin Films VI* (Vol. 8818, p. 881803). International Society for Optics and Photonics.

[24] Cheng, F., Gao, J., Luk, T. S., & Yang, X. (2015). Structural color printing based on plasmonic metasurfaces of perfect light absorption. *Scientific reports*, *5*, 11045.

[25] Scarpa, F., & Tomlinson, G. (2000). On static and dynamic design criteria of sandwich plate structures with a negative Poisson's ratio core. *Applied Mechanics and Engineering, 5*(1), 207-222.

[26] Scarpa, F., & Tomlin, P. J. (2000). On the transverse shear modulus of negative Poisson’s ratio honeycomb structures. *Fatigue & Fracture of Engineering Materials & Structures, 23*(8), 717-720.

[27] Lee, H. T., Kim, M. S., Lee, G. Y., Kim, C. S., & Ahn, S. H. (2018). Shape memory alloy (sma)-based microscale actuators with 60% deformation rate and 1.6 kHz actuation speed. *Small, 14*(23), 1801023.

[28] Wan, H., Ohtaki, H., Kotosaka, S., & Hu, G. (2004). A study of negative Poisson's ratios in auxetic honeycombs based on a large deflection model. *European Journal of Mechanics-A/Solids, 23*(1), 95-106.

[29] Li, D. Y. (2000). Exploration of TiNi shape memory alloy for potential

application in a new area: tribological engineering. *Smart materials and structures, 9*(5), 717.

[30] Seo, J., Kim, Y. C., & Hu, J. W. (2015). Pilot study for investigating the cyclic behavior of slit damper systems with recentering shape memory alloy (SMA) bending bars used for seismic restrainers. *Applied Sciences, 5*(3), 187-208.

[31] Chan, W. L., Chen, H. T., Taylor, A. J., Brener, I., Cich, M. J., & Mittleman, D. M. (2009). A spatial light modulator for terahertz beams. *Applied Physics Letters*, *94*(21), 213511.

초록

형상기억합금 기반의 변형가능한 어그제틱 플라즈모닉 메타물질

임종혁

서울대학교 기계공학부 대학원

금속 나노구조체의 표면 플라즈몬 공명은 독특한 전자기 특성으로인해 지금까지 꾸준한 관심을 끌고있다. 특히, 입사광의 파장보다 작은 크기의 전도성 나노 입자, 나노 구조체로 빛이 입사할 때 발생하는 국소 표면 플라즈몬 공명은 파장 흡수기, 색 필터 및 센서 등에 적용돼 왔다. 이는 공진 주파수가 나노 구조체의 크기, 형상 또는 주위의 유전체 특성에 따라 달리 결정되기 때문이다. 그러나, 이전까지의 연구에서 개발된 플라즈모닉 물질들은 고정된 구조에서 벗어나지 못해 공진 주파수를 연속적으로 변경시킬 수 없다는 한계를 가지고 있다. 이 문제는 플라즈모닉 메타물질의 실제적 적용에 어려움을 주었다.

이번 연구에서는, 가시광 영역에서 공명 주파수를 이동시킬 수 있는 어그제틱 나노 패턴이 새겨진 플라즈모닉 메타물질이 개발되었다.

이 메타물질은 직경이 25 μm인 형상기억합금 와이어로 제작되어 패턴이 인장되고 열에 의해 복원될 수 있다. 이러한 메타물질을 제작을 위해서 집속이온 빔을 이용하여 1 μm 두께의 형상기억합금 필름을 제작했고, 뛰어난 기계적 물성을 가진 어그제틱 패턴을 그 위에 새겼다. 이후, 이온 코터 스퍼터링과 전자빔 증착방식을 사용하여 패턴위에 금과 은 나노입자를 증착하였다. 패턴의 인장을 위해서는 마이크로 그리퍼를 사용하였으며, 인장 후 355 nm 레이저를 이용하여 패턴을 원래의 형상으로 되돌릴 수 있었다. 패턴 크기의 변화에 따른 반사 효과를 확인하기 위해, 우리는 스펙트로미터를 이용한 흡수픽을 측정했을 뿐만 아니라, 광학현미경을 통해 직접 색을 확인했다. 또한, finite difference time domain (FDTD) 방식을 이용하여 동일한 모델에 대해 반사율을 계산했고 그 결과를 실험결과와 비교했다.

위와 같은 실험을 통해, 먼저 여러가지 패턴의 크기에 따라 다양한 색이 나타나는 것을 확인했다. 또한 패턴을 잡아당겨 그 크기를 약 10% 까지 늘렸을 때, 흡수픽이 이동하고 반사색이 변화하는 것을 확인했다. 최종적으로, 형상기억효과를 이용하여 원래의 패턴크기로 되돌림으로서 변형가능한 어그제틱 플라즈모닉 메타물질을 증명했다.

주요어: 표면 플라즈몬 공명, 형상기억합금, 어그제틱, 메타물질, 플라즈모닉

학번: 2018-26302

creative commons
COMMONS DEED

저작자표시-비영리 2.0 대한민국

이용자는 아래의 조건을 따르는 경우에 한하여 자유롭게

- 이 저작물을 복제, 배포, 전송, 전시, 공연 및 방송할 수 있습니다.
- 이차적 저작물을 작성할 수 있습니다.

다음과 같은 조건을 따라야 합니다:

저작자표시. 귀하는 원저작자를 표시하여야 합니다.

비영리. 귀하는 이 저작물을 영리 목적으로 이용할 수 없습니다.

- 귀하는, 이 저작물의 재이용이나 배포의 경우, 이 저작물에 적용된 이용허락조건을 명확하게 나타내어야 합니다.
- 저작권자로부터 별도의 허가를 받으면 이러한 조건들은 적용되지 않습니다.

저작권법에 따른 이용자의 권리는 위의 내용에 의하여 영향을 받지 않습니다.

이것은 이용허락규약(Legal Code)을 이해하기 쉽게 요약한 것입니다.

Disclaimer

dCollection

공학석사학위논문

형상기억합금 기반의 변형가능한 어그제틱 플라즈모닉 메타물질

Shape memory alloy-based deformable auxetic plasmonic metamaterials

2020 년 8 월

서울대학교 대학원

기계공학부

임 종 혁

Abstract

Shape memory alloy-based deformable auxetic plasmonic metamaterials

Jong-Hyuk Im

Department of Mechanical Engineering

The Graduate School

Seoul National University

Surface plasmon resonance of metallic nanostructures has attracted steady attention for their distinct electromagnetic properties. In particular, localized surface plasmon resonance (LSPR) occurs when light enters conductive nanostructures or nanoparticles smaller than the incident wavelength has been applied to wave absorbers, color filters, and sensors. This is because the resonant frequency can be determined depending on the size, geometry, and dielectric environment of the structures. However, the plasmonic materials developed in the previous researches have a limitation that the resonant frequency could not be changed continuously due to their stationary structure. This problem makes it difficult for practical applications.

In this research, we develop plasmonic metamaterials with auxetic nano patterns that can shift the resonant frequency in the visible region. Shape memory alloy (SMA) wire with 25 μm diameter is used to stretch the patterns and bring them back. Using focused ion beam (FIB), 1 μm thick SMA thin film is fabricated from wire, and the auxetic nano patterns showing remarkable mechanical property are engraved on the film. Gold and silver nanoparticles are sputtered onto the patterned thin film using an ion coater sputtering and e-beam evaporation. We use a micro-gripper to stretch the patterns, and patterns are returned to its original shape by 355 nm laser. To confirm the effect of changing the size of patterns, we not only measure the absorption peak through the spectrometer but also observe the color directly through the microscope. Besides, the finite difference time domain (FDTD) method is used to calculate the reflectance and compare with the experimental results.

Through the above experiment, it is confirmed that various colors appeared depending on the size of auxetic patterns. Also, when the pattern is pulled to increase the size to about 10%, it is measured that the absorption peak moved and the reflection color changed. By returning to the original pattern size using the shape memory effect, deformable auxetic plasmonic metamaterials are demonstrated.

Keywords: Localized surface plasmon resonance, Shape memory alloy, Auxetic, Metamaterials, Plasmonic

Student Number: 2018-26302

Table of Contents

List of Figures

List of Tables

Chapter 1. Introduction

In general, most materials are known to have unalterable intrinsic properties such as chemical, mechanical and optical characteristics. However, when the bulky materials are divided into several nanometers to hundreds of nanometers in size, it exhibits different characteristics from the mass material. This is related to the intermolecular orbit, because the smaller the particle, the more irregular the electron orbit, resulting in a discontinuous energy level - a bandgap. Optically, this bandgap absorbs, scatters, and diffracts light through interaction, allowing control the wavelength of reflection and transmission. As this unique property of nanostructures has been discovered, and as micro-processes have been developed, research on the nanostructures have been conducted in various fields for use as structural color, wavelength absorber, optical sensor, metamaterials, etc.

There are many principles in which nanostructures generate their unique optical properties. Quantum dots, which have been actively researched recently, use photo-luminescence and electro-luminescence. The wavelength range of emission varies depending on the size of the quantum dot. [1] Another major factor is surface plasmon resonance. The plasmons on the metal surface strongly increase absorption and scattering by interacting with the specific energy of the incident light. This effect causes a subtractive color. [2] Diffraction grating has a periodic structure, which splits incident light spatially and diffracts in different directions to generate a color. [3] The thin film multi-layer method selectively absorbs light from a specific wavelength region by using interference. [4] As such, various methods of altering the spectrum of light have been studied.

Among them, metamaterials based on localized surface plasmon resonance (LSPR) which occurs when light enters conductive nanostructures or nanoparticles smaller than the incident wavelength have a great advantage. This is because the

profile of reflected light can be adjusted simply by altering the size, shape, and material of the nanostructure. Besides, resonance occurs at the same wavelength regardless of the angle of the incident light. For these reasons, researches on the optical properties of LSPR has been steadily conducted. [5-7]

However, the LSPR-based metamaterials developed so far have been not tunable in that they use a fixed nanostructure. So, the spectrum could not be continuously adjusted. These lead to the difficulty of producing structures of various shapes and sizes to obtain diverse spectrums.

Here, we develop plasmonic metamaterials that can continuously control the resonance frequency in the visible light region through mechanical actuation. Shape memory alloy (SMA) is used to deform the pattern and restore the original shape by the shape memory effect (SME). The auxetic structure used for patterning has excellent mechanical properties and unique electromagnetic properties. [8] This auxetic structure is based on the re-entrant honeycomb design and has a negative Poisson's ratio, which simultaneously increases the length in the vertical direction during horizontal tension. This increases the size of the overall pattern and makes the absorption peak move clearly. Patterning is performed by using focused ion beam (FIB), and the LSPR effect was enhanced as much as possible by sputtering gold and silver particles. The reflectance before and after the tension is measured using a spectrometer, and also analyzed and compared using a finite-difference time-domain (FDTD) method. Finally, materials that actively shift the absorption peak based on SMA is explored.

Chapter 2. Background

Nanostructures have unique optical properties that do not occur in bulk materials, such as scattering, propagating, absorbing, diffracting or mix of them through interactions with light. LSPR uses scattering and absorbing among them. This chapter provides the principle of LSPR that control the spectrum of light from visible light to infrared. We also examine the pros and cons of this principle and briefly look at the progress of the studies so far. Finally, we find out how these principles work in a complex way and also present the industrial applications of each principle.

2.1. Localized surface plasmon resonance

Surface plasmon resonance (SPR) is a phenomenon in which conductive electrons on a metal surface and external light resonate under certain conditions. Usually, SPR occurs at a specific angle of incident light and greatly increases the absorptance of the metal surface. It is often used as a biosensor to identify the composition of the materials adsorbed on the substrates. [9]

By the way, when the metal nanoparticles or nanostructures smaller than the wavelength of the incident light collide with the phonon, electromagnetic properties are enhanced locally. At this time, the absorption peak shifts according to the size and shape of nanoparticles, nanostructures, not angles, which is called localized surface plasmon resonance. In particular, silver and gold nanoparticles greatly increase this effect. [10,11].

2.2. Applications of localized surface plasmon resonance

LSPR-based nanostructures do not change the resonance energy by the angle of the incident light, which is a representative advantage of LSPR. The area that can maximize this property is coloration. The use of LSPR in the visible light region can produce subtractive colors by absorption of light, which is notable in the field of coloration because it can minimize the color change according to the viewing angle. In fact, this method has been used since ancient Roman times. The evidence is the Lycurgus Cup, a Roman work of art exhibited at the British Museum. (Figure 1) Another example is a stained-glass window representing the Gothic cathedral in the Middle Ages. (Figure 2) The stained glass uses different resonant energy depending on the size of the gold and silver nanoparticles. Figure 2 shows where the colors for gold and silver particles of less than 100 nm are used respectively.

A wave absorber is a practical application in which the most basic characteristics of controlling the electromagnetic wave of LSPR are used. Landy *et al.* developed a perfect wave absorber with an absorptivity of up to 99% using the three-layer called metal-insulator-metal (MIM) structure. (Figure 3)

Application to selective thermal emitters has also been attempted, based on Kirchhoff's thermal radiation law that emissivity and absorptivity of materials are the same. (Figure 4) In this paper, through the microstrip patch array, it was possible to observe the strong heat emission of the same type as the light absorption by SPR at a specific wavelength. In addition, researches have been conducted for use as a detector or sensor using the feature that the operating wavelength can be controlled using the size or shape of the nanostructure. [12, 13]

However, the color using LSPR has low vibrancy. Also, there is a limitation that only metal must be used for the plasmon resonance characteristics, so it is onerousness to produce another structure to control the absorption wavelength band.

Figure 1. The Lycurgus Cup [14]

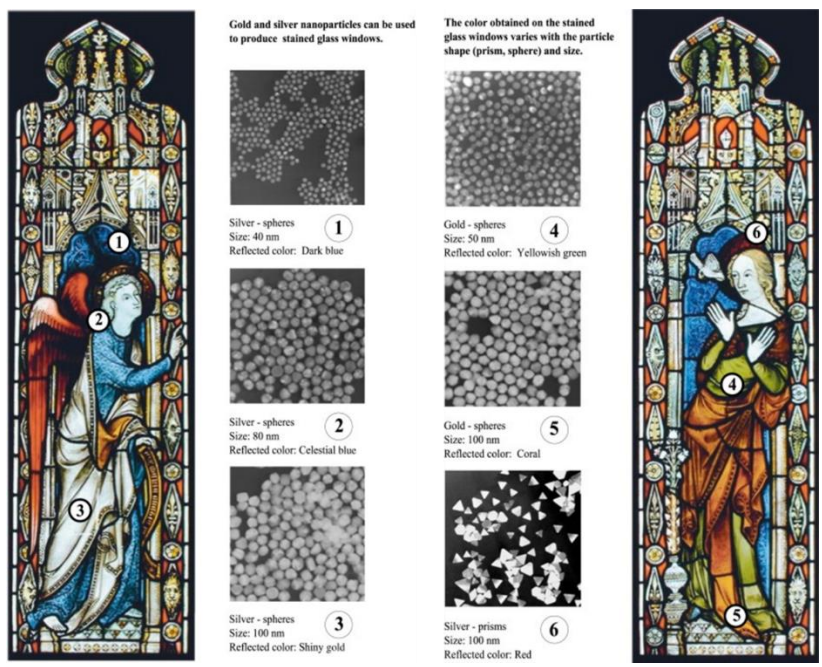

Figure 2. Effect of nanoparticles on the colors of the stained glass windows [15]

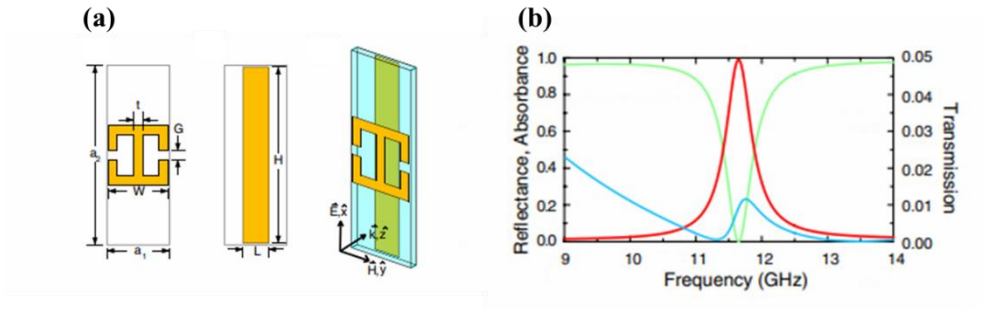

Figure 3. The first developed metamaterial perfect absorber. (a) top layer view, cut wire view, and a perspective view. (b) simulated R(ω) (green), A(ω) (red), T(ω) (blue) [16]

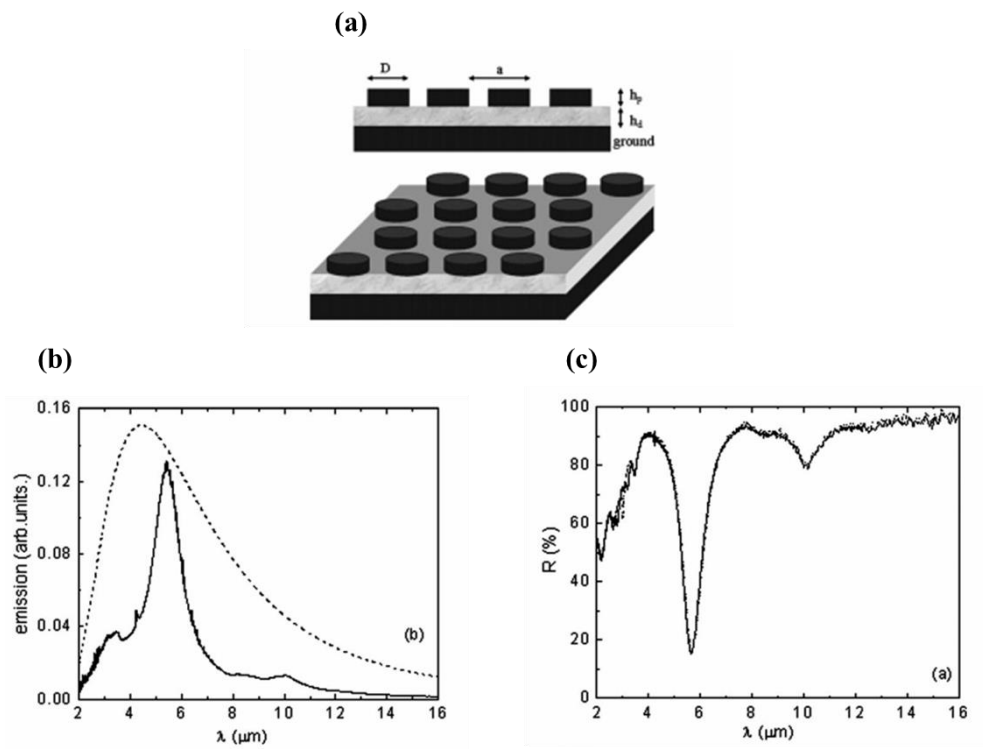

Figure 4. The first developed metamaterial thermal emitter. (a) hexagonal array of circular patches (b) emission (c) reflectivity [17]

2.3. Comparison with other principles

In nano optics, there are various principles that generate unique optical properties. It is necessary to identify each feature to fit the ability required in various fields, and it is shown in Figure 5. The absorber based on the localized surface plasmon resonance uses metal nanoparticles or nanostructures of several nanometers to hundreds of nanometers, so it has good spatial resolution and angle independency but has a poor full width at half maximum (FWHM) characteristics of the absorption spectrum, so the clarity of absorption peak is relatively inferior. Thin film interference-based materials use absorption characteristics in the spectral band as well, but the peak intensity is clear, so the vibrancy of the color is good. However, the reflection spectrum is not constant according to the viewing angle. Diffraction pattern, nanohole array, and other photonic structure reflect only a specific wavelength region, and as with thin film interference, clarity of color is good but it depends on angle.

In fact, these working principles are mostly not used alone. Researchers use a mixture of properties to compensate for the shortcomings of each property, the most important of which is the plasmon on the metal surface. A plasmon is the collective oscillations of free conduction electrons in metals that interact with the specific energy of the incident light according to the surface structure in the dielectric environment. Through interaction, the surface of the metal is electrically polarized to induce a strongly amplified electromagnetic field, and it greatly increases absorption and scattering. One of the most active areas of surface plasmon research is coloration. Various research has been carried out on plasmonic structural color which uses the subwavelength scale effect using EBL and FIB to engrave periodic patterns on the metal film. [18-21] The plasmonic effect is also used in a multi-layer structure by making patterns on the top layer. As such, the surface plasmon has been studied by overlapping with other principles besides itself due to the effect of amplifying the electromagnetic field. (Table 1)

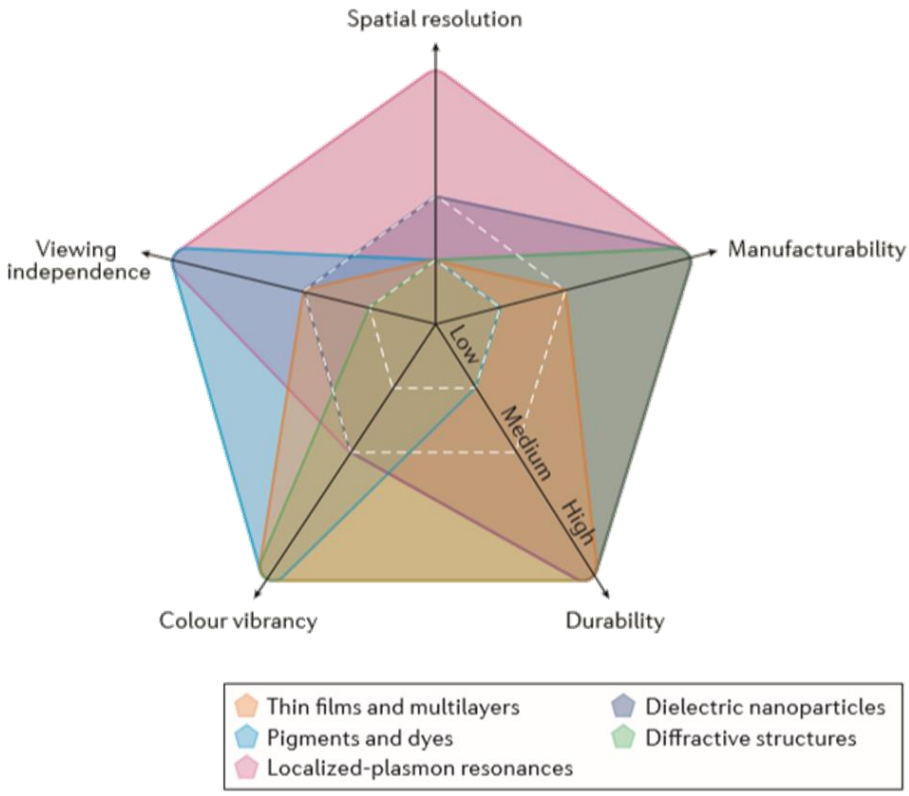

Figure 5. Performance indicators of various nanostructures [22]

Table 1. Types of plasmonic color filter

Diffraction grating	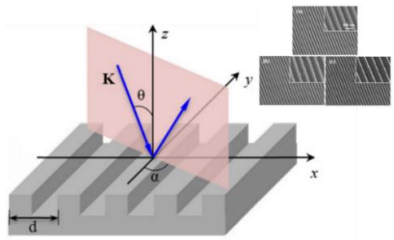 [18]	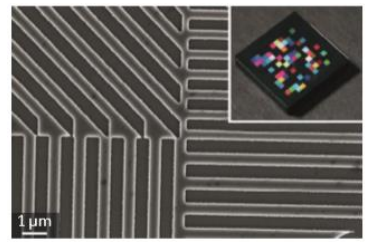 [23]
Nanohole array	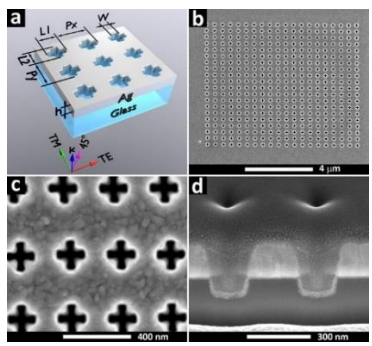 [19]	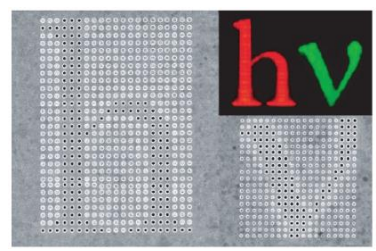 [20]
Multi-layer	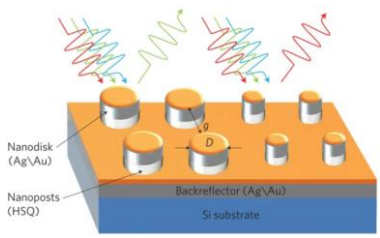 [21]	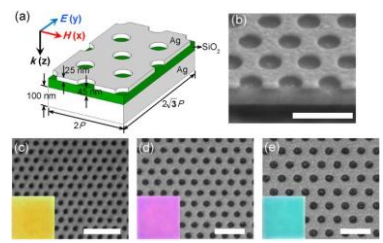 [24]

Chapter 3. Design, fabrication process, experimental setup

This chapter introduces the design, fabrication process, and experimental setup. Shape memory alloy was used for the deformability of the patterns and its type is Nickel-Titanium alloy (nitinol) wire. A nitinol thin film was fabricated using FIB and an auxetic structure called Re-entrant honeycomb was engraved on the thin film. This auxetic structure has a negative Poisson's ratio, and we aimed at a value of -1 to maximize the perpendicular direction of the tensile, leading to a dramatic change in the size of the structure. The thickness of the pattern was determined by considering nitinol's machinability and stability of deformation. After pattern processing, gold and silver thin films were deposited via ion sputtering coater and e-beam evaporation equipment to enhance the LSPR-based absorption effect in the visible region. Through a system comprised of the LED light source, VIS spectrometer, and the optical microscope, the reflectance of the fabricated material was measured in the range of 420 nm to 680 nm and subtractive colors were confirmed. Micro tweezer was used to tension the patterns and a laser with UV wavelength was used for shape memory effect. Section 3.1 introduces the design of the patterns, then the fabrication process and experimental setup are described in sections 3.2 and 3.3, respectively.

3.1. Design of auxetic pattern

The design of the patterns was inspired by the shape of the re-entrant honeycomb. (Figure 6) This form, commonly called the auxetic structure, has been studied in many ways because it has a negative Poisson ratio that is not visible naturally. Geometrically, researches on axial stiffness and bending behavior of auxetic structure demonstrated excellent indentation and buckling resistance of auxetic structure that enables stable tension. [25,26] In addition, this structure is shown to have unique characteristics electronically that have an effective permittivity, which is biaxially anisotropic. [8]

Although the excellent mechanical properties of the auxetic structure had been revealed as described above, we wanted to identify the actual tensile properties of nitinol, not mathematical calculations. A microscale auxetic actuator was manufactured using nitinol wire as shown in Figure 7 (a), and its performance was evaluated in comparison with the previous studies. [27] The tensile force according to the strain was measured via a micro force sensor, and the tensile length was sequentially increased. As a result, it was confirmed that stable tension is possible at a lower stress than the existing diamond-type actuator. (Figure 7. (b))

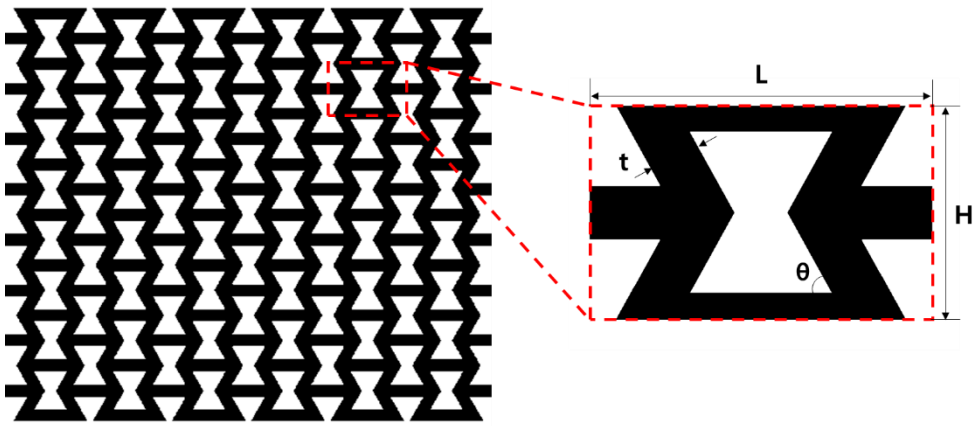

Figure 6. Re-entrant honeycomb auxetic structure

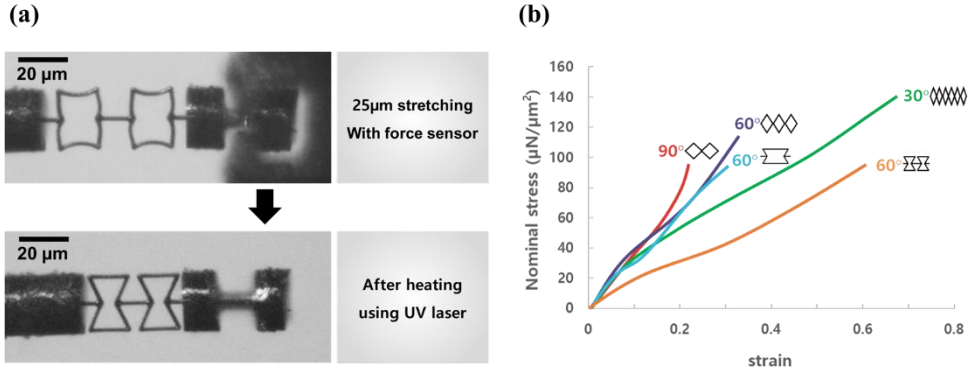

Figure 7. (a) SMA-based micro scale auxetic actuator (b) stress -strain curve of SMA-based micro actuator [27]

Another feature of the auxetic structure is that it has a negative Poisson's ratio. That is, the pattern deformation can be maximized by increasing not only the direction in which the patterns are pulled but also the vertical direction. This property is suitable for this experiment because the absorption peak shifts depending on the size of the deformed pattern. According to previous research, the Poisson's ratio of the auxetic structure depends on the height (H), length (L), and internal angle (θ) shown in Figure 6. [28] The results of the research are shown in Figure 8. Based on this table, the size of the H/L and the internal angle were determined so that the Poisson's ratio would be -1. Figure 9 is nano patterns actually fabricated, and surface plasmon resonance occurs in the infrared region and visible region respectively.

	H/L		1.5	2	2.5	3	3.5	4
λ	$\pi/18$	ν_X	−4.211	−3.058	−2.40	−1.976	−1.679	−1.460
	$\pi/9$		−2.230	−1.557	−1.196	−0.971	−0.818	−0.706
	$\pi/6$		−1.5	−1	−0.75	−0.6	−0.5	−0.429
	$2\pi/9$		−1.065	−0.673	−0.492	−0.387	−0.320	−0.272
	$5\pi/18$		(−0.735)	−0.437	−0.311	−0.241	−0.197	−0.167
	$\pi/3$		(−0.455)	−0.255	−0.177	−0.135	−0.110	−0.092

Figure 8. Poisson's ratio of auxetic structure at small deformation [28]

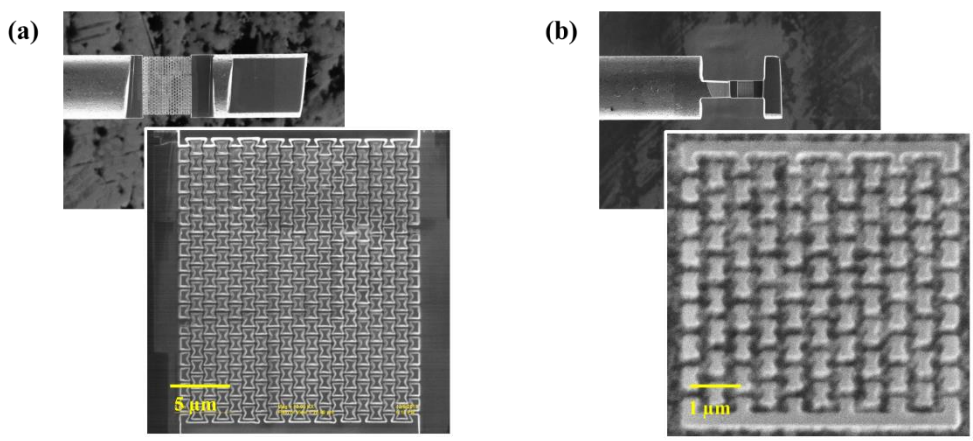

Figure 9. SED image of auxetic structure (a) infrared region (b) visible region

3.2. Fabrication process

The process of cutting and patting nitinol via FIB was developed. The nitinol used in this experiment is a shape memory alloy composed of 50% nickel and titanium, and phase transformation occurs at 70 °C, making it relatively resistant to heat. (Dynalloy, Inc., Costa Mesa, CA, USA) The detailed characteristics are in Table 2, and the SMA phase transition process is illustrated in Figure 10. This nitinol is a smart material that reacts to heat reversibly and has high biocompatibility, thus giving the possibility of being used in a diversity of fields. [29]

Table 2. Nitinol physical properties

Density		**6.45 g/cm^3**
Specific Heat		**0.2 cal/g × °C**
Melting Point		**1300 °C**
Latent Heat of Transformation		**5.78 cal/g**
Thermal Conductivity		**0.18 W/cm × °C**
Transition Temperature		**70 °C**
Poisson Ratio		**0.33**
Thermal Expansion Coefficient	**Martensite**	**6.6×10^{-6} /°C**
	Austenite	**11.0×10^{-6}/°C**
Electrical Resistivity	**Martensite**	**80 micro-ohms × cm**
	Austenite	**100 micro-ohms × cm**

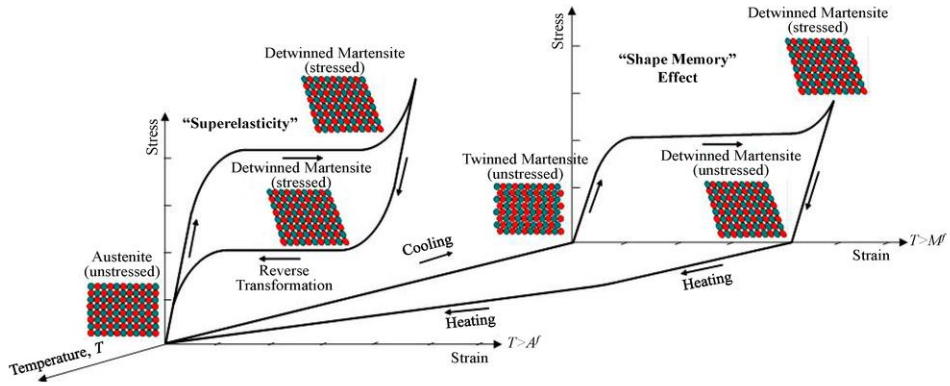

Figure 10. Phase transition of shape memory alloy [30]

Figure 11 shows the overall process for fabricating SMA-based plasmonic metamaterials. The first step is to cut SMA thinly via FIB to produce about 1 μm thickness of the film. Subsequently, the patterning was also performed with FIB after rotating the specimen by 90 degrees. At this time, the patterns were carved with an interval of about 15 nm to identify the change of absorption peak according to the size of the auxetic structure and to see the subtractive color. Later, gold and silver nano film were deposited via ion sputtering coater and e-beam evaporation equipment. This is because the FDTD analysis demonstrated that thickness of more than 50 nm is not very helpful in improving reflectivity. (Figure 12)

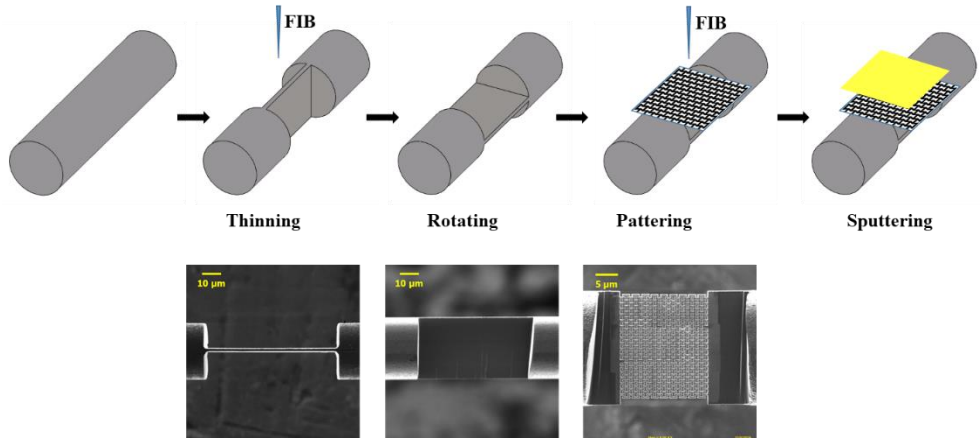

Figure 11. Fabrication process of SMA-based plasmonic metamaterials

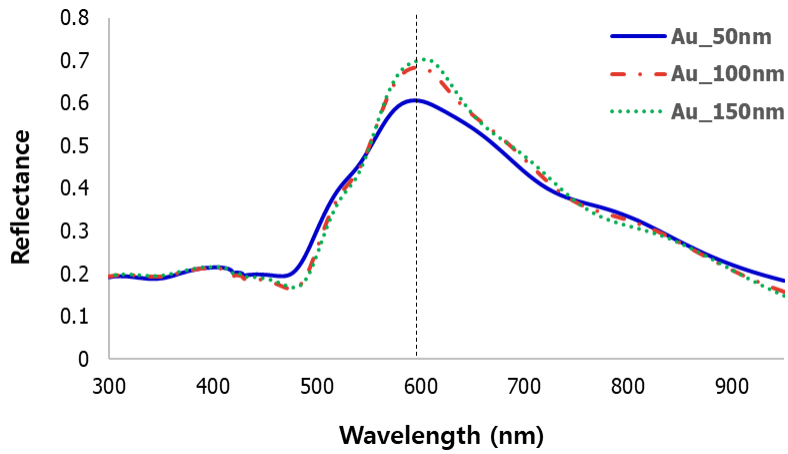

Figure 12. Reflectance of auxetic plasmonic materials with gold film thickness via FDTD method

3.3. Experimental setup

This section introduces an experimental setup dealing with plasmonic metamaterials. The overall form is shown in Figure 13. An upright microscope (BX53MTRF-S, Olympus, Tokyo, Japan) was used to observe the reflected image. A spectrometer (FLAME-S-UV-VIS, Ocean Optics, Largo, USA) was coupled to a microscope to measure the spectrum reflected when LED light was incident. The manual controller and Automatic controller were used for the operation of the 3-axis nano stage. In order to confirm the change in the absorptance during tension, the metamaterial sample for measurement and a microgripper were respectively coupled to two 3-axis nano stages, and detailed form is shown in Figure 14. Finally, a control platform was constructed that can simultaneously measure spectral data while observing the images through a microscope.

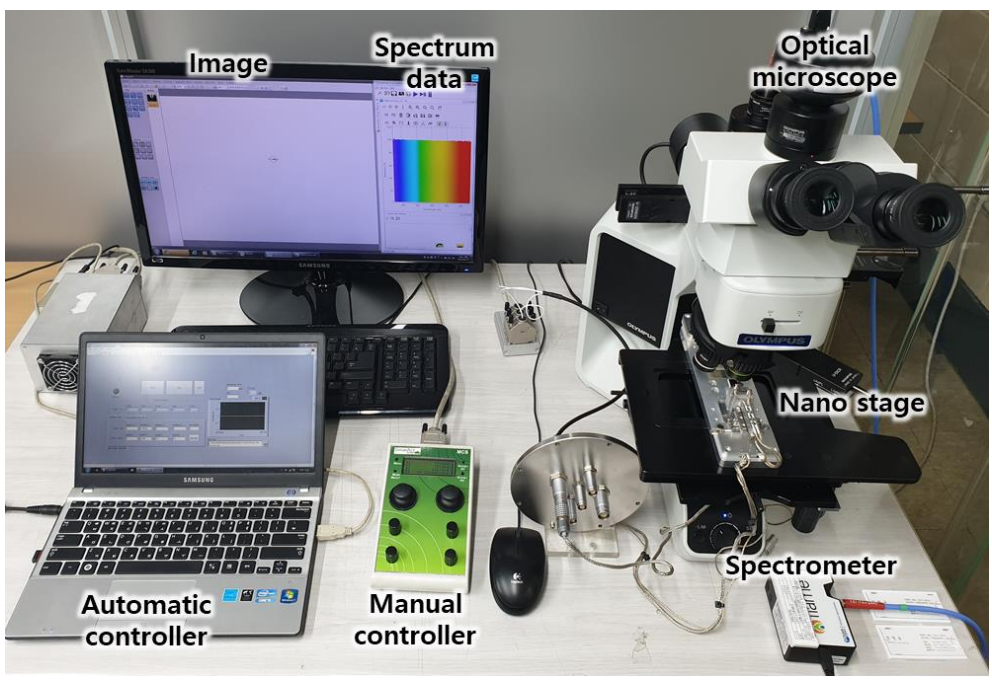

Figure 13. Experimental setup for spectrum measurement

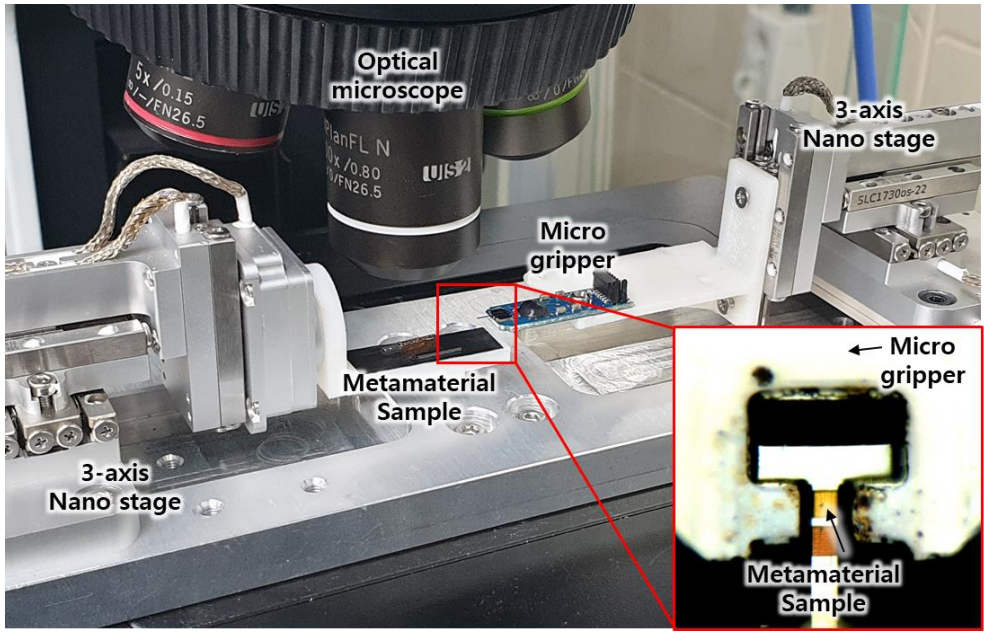

Figure 14. Control platform for tensile test

Chapter 4. Localized surface plasmon resonance depending on the auxetic pattern size

In this chapter, we introduce the change in absorption wavelength according to the auxetic pattern size of developed metamaterials. The size of the auxetic patterns was determined to cause localized surface plasmon resonance in the visible wavelength region. Also, the overall shape of auxetic patterns was maintained although the size was changed.

First, in order to confirm the position of the absorption peak according to the size of the patterns, several patterns with specific intervals were produced. Then, we sputtered silver and gold film on the fabricated patterns. In this process, we also confirmed the excellent LSPR effect of silver and gold film by comparing before and after the deposition of these metal films. Lastly, in each case, the reflective color was observed through an optical microscope, and the experimental results were verified by comparing the measured spectral data and the simulated data from FDTD.

4.1. The influence of Ag film in LSPR

The shape memory effect of nitinol is differentiated from other metals, enabling tension and recovery of patterns. However, as explained in the previous chapter, nitinol is known to have a relatively weak LSPR effect in the visible region compared to silver and gold. This section demonstrated that difference by comparing the reflection spectrum of patterns made only with nitinol and patterns deposited with silver.

The picture to the right of Figure 15 shows the metamaterials that were fabricated. For the tension of the pattern, the shape of the entire sample was made to match the shape of a micro tweezer. A spectrum of vertical reflectance with LED light was measured before and after the deposition of Ag film and observed through an optical microscope. The results are shown in the graph on the left. The graph shows the reflection spectrum for before and after Ag deposition for the top pattern in the photo on the right. In both cases, the positions of the absorption peaks were the same, but as a whole, they were more pronounced after deposition. In addition, this result could be confirmed by the reflection color in the picture on the right. This was the same for Au, and thus, the production of metamaterials was completed by laminating about 50 nm silver and gold thin film through e-beam evaporation and ion coater sputtering respectively.

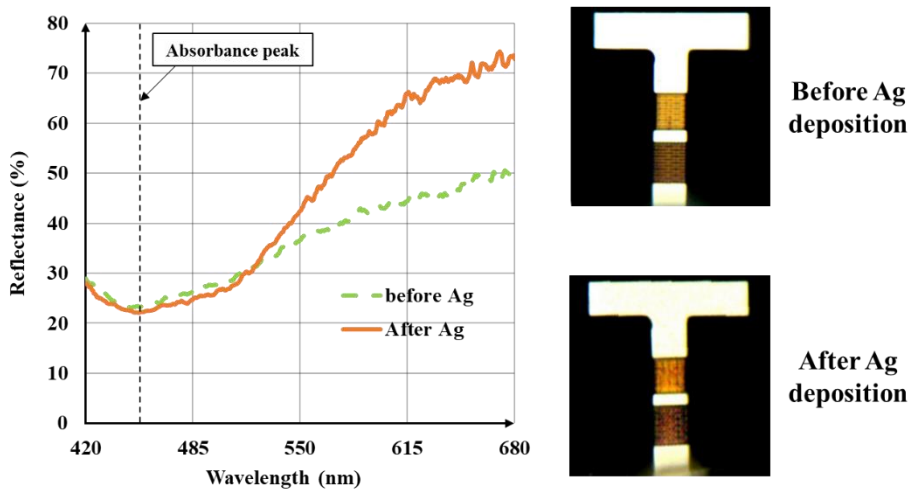

Figure 15. Before and after Ag thin film deposition (a) reflection spectrum (b) image from optical microscope

4.2. Reflectance depending on the pattern size with Ag film

The metamaterials developed in this research are based on LSPR, so the wavelength range in which light absorption occurs varies depending on the size or shape of the patterns. As shown in Figure 16, SMA-based auxetic patterns of different sizes were produced via FIB. After FIB processing, Au and Ag thin films were deposited on the patterns to amplify the absorption effect, as demonstrated in the previous section. First, this section shows the experimental results when Ag thin films were laminated.

The spectrometer measurement results and optical microscopy images of metamaterials with about 50 nm Ag film are shown in Figure 17. Each pattern on the right side of Figure 17 forms a size ranging from 500 nm × 810 nm to 650 nm × 1080 nm based on the height × width of the auxetic pattern shape in Figure 6. The measurement wavelength area is from 430 nm to 680 nm, which is close to the general visible light range, and the plasmon resonance of the patterns that occurred in this area. As a result, maximum light absorption of each pattern occurs at (a) 450 nm, (b) 500 nm, (c) 545 nm, (d) 575 nm, and (e) 610 nm. The overall tendency is that as the size of the pattern increases, the absorption wavelength region also increases, which proves that the localized surface plasmon resonance phenomenon is occurring.

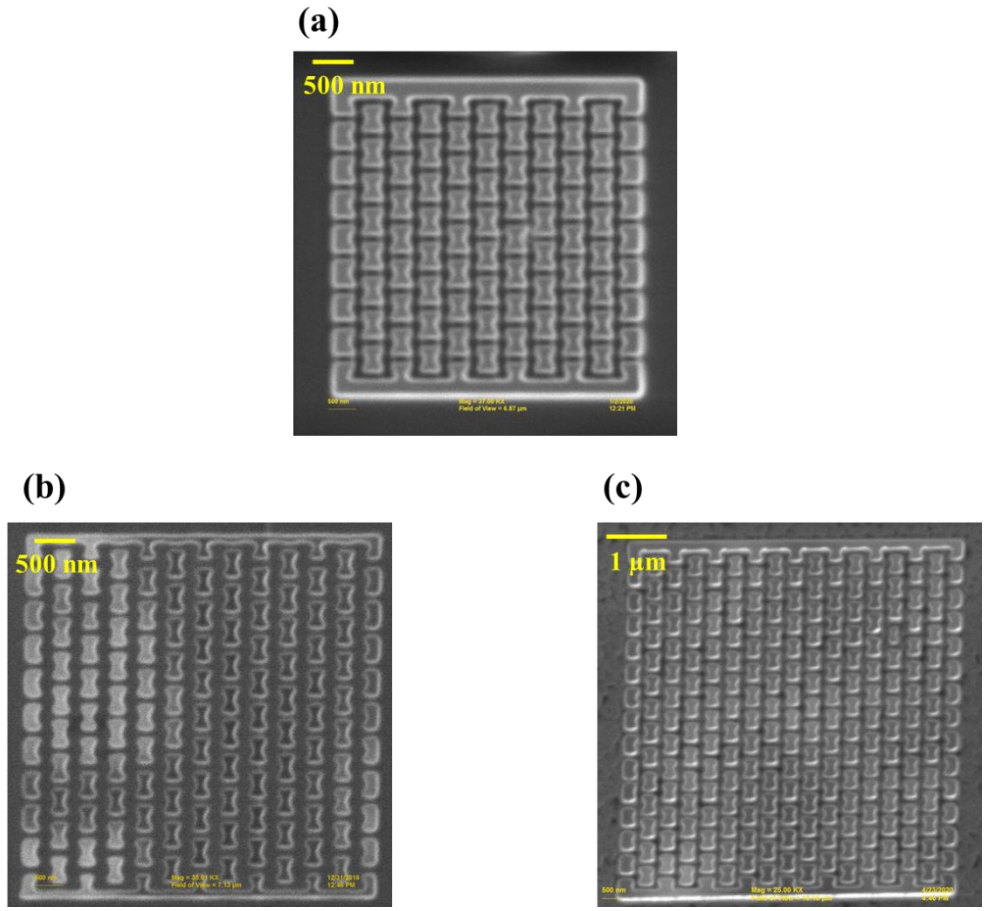

Figure 16. SED image of different sized auxetic patterns
(a) 500 nm × 810 nm, (b) 550 nm × 900 nm, (c) 585 nm × 965 nm

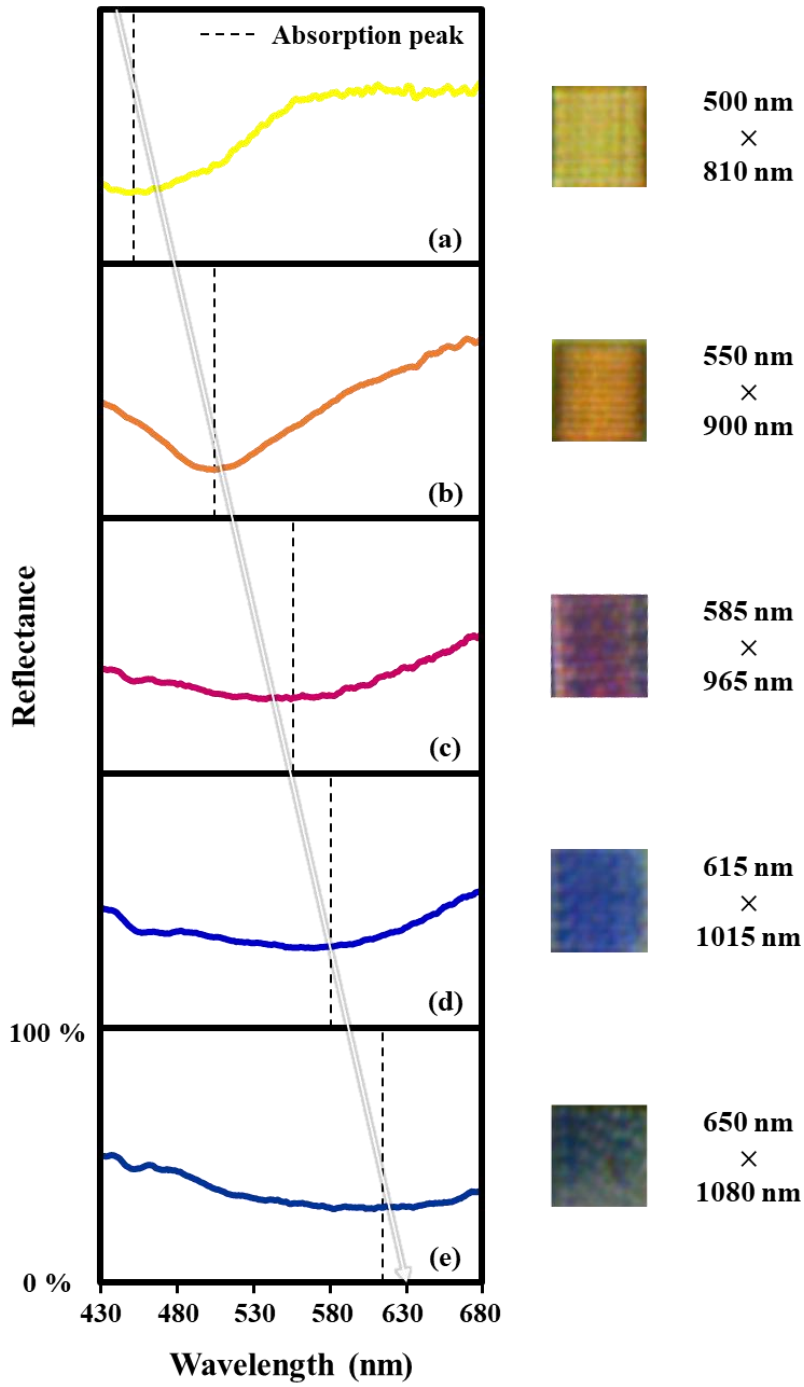

Figure 17. Reflectance and microscopy image under varying the patterning size. The maximum absorption occurs at (a) 450 nm, (b) 500nm, (c) 545 nm, (d) 575 nm (e) 610 nm

To prove the actual experimental results, 3D models of the same shape were depicted to obtain reflectance data for vertical reflection of light through the FDTD method. The modeling is shown in Figure 18. For the silver film, the refractive index of CRC was used, and in the case of nitinol, the refractive index ($\tilde{N} = n - jk$) actually measured using ellipsometry was used. In the analysis area of the FDTD, the boundary condition of the sides was selected as symmetry and anti-symmetry condition so that the same auxetic pattern is periodically replicated infinitely. In addition, perfectly matched layer (PML) boundary was adopted for the top and bottom surfaces so that 100% of the light is absorbed when it touched, so as not to affect within the analysis area. The results are shown in Figure 19. The absorptions were maximum at (a) 455 nm, (b) 510 nm, (c) 545 nm, (d) 565 nm, and (e) 600 nm, respectively. There was only an error up to 10 nm wavelength compared with experimental results. Also, the absorption peak can be clearly observed in the simulation results than the actual experiments.

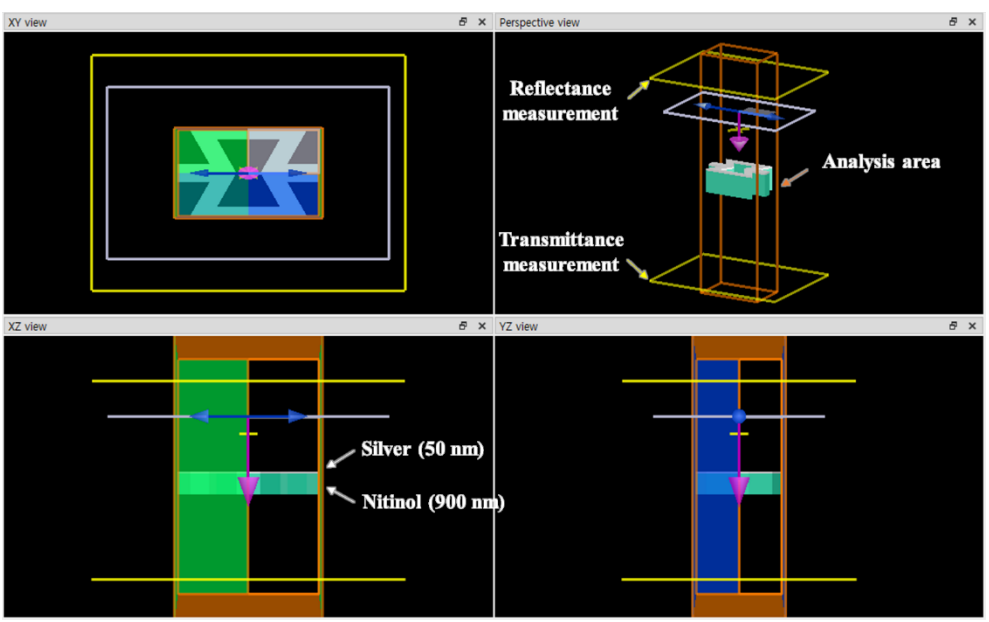

Figure 18. Finite difference time domain image of auxetic metamaterials

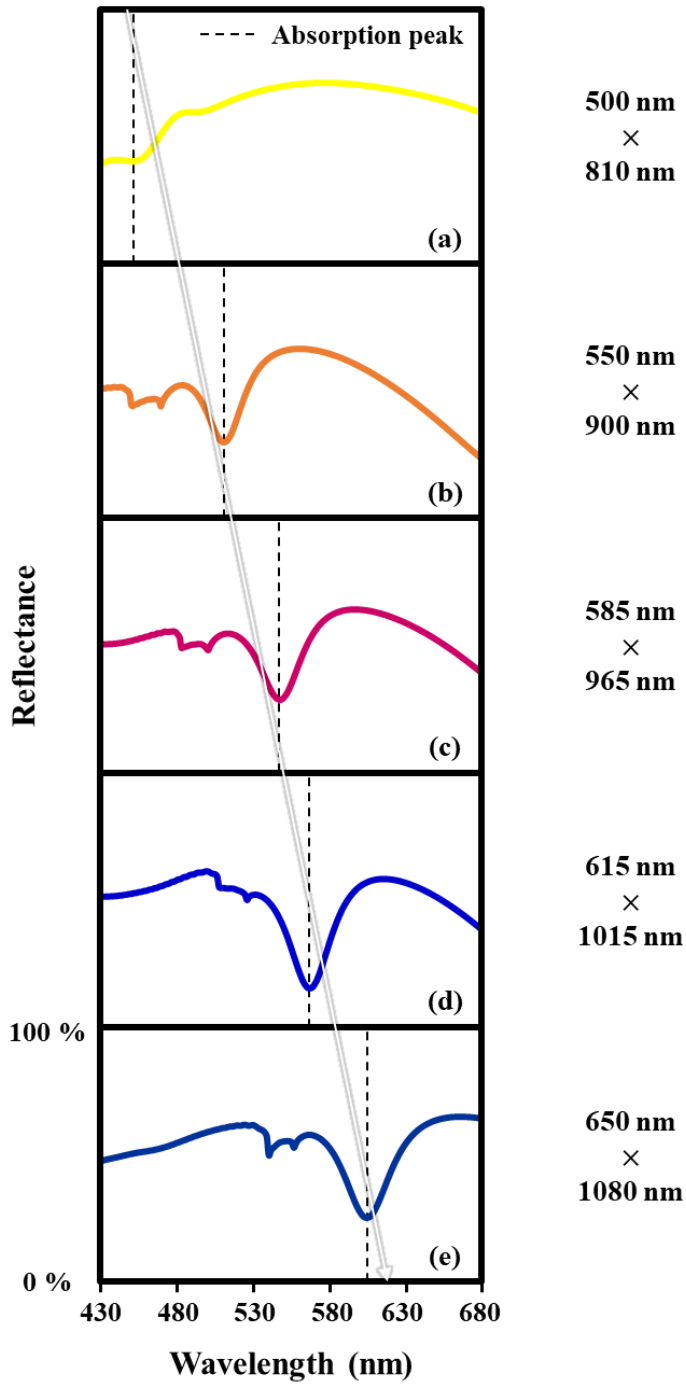

Figure 19. Reflectance via FDTD under varying the patterning size. The maximum absorption occurs at (a) 455 nm, (b) 510nm, (c) 545 nm, (d) 565 nm (e) 600 nm

4.3. Reflectance depending on the pattern size with Au film

Like the silver film, the gold film is also a metal that maximizes the LSPR phenomenon in the visible area. In order to confirm the LSPR effect of gold film, we introduce the change of reflectance according to the size of the pattern when the gold thin film is deposited on metamaterials engraved with auxetic pattern fabricated by using FIB. At this time, the gold film was deposited about 50 nm through an ion sputtering coater.

The actual measured reflection spectrum and color according to the pattern size are shown in Figure 20. For pattern sizes from 500 nm × 810 nm to 650 nm × 1080 nm, as the overall pattern size of the reflectance increases, the position of the absorption peak tends to increase. The positions of the absorption peaks are (a) 445 nm, (b) 530 nm, (c) 570 nm, and (d) 620 nm. However, the gold film, unlike silver, has a very low reflectance in the blue region (~ 485 nm). Therefore, it was difficult to observe the CMY colors, and the colors related to blue were not found. Therefore, in the next chapter's tensile test, a silver film was deposited to confirm the color change using all colors.

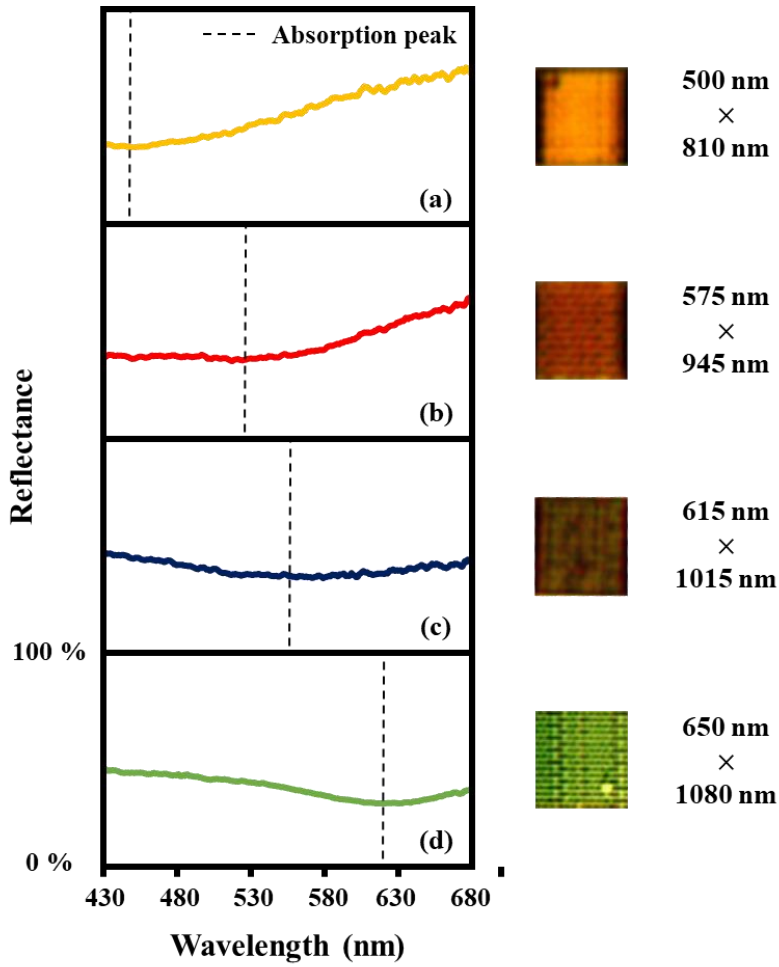

Figure 20. Reflectance and microscopy image under varying the patterning size. The maximum absorption occurs at (a) 445 nm, (b) 530nm, (c) 570 nm, (d) 620 nm

Chapter 5. Localized surface plasmon resonance of pattern under tension loading

This chapter introduces an experiment that stretches the patterns and shifts the wavelength where the LSPR phenomenon occurs as its size increases. As confirmed in the previous section, in the case of gold film, the reflectance is not sufficiently high below the blue wavelength (~ 485 nm), so that the corresponding color and absorption spectrum results cannot be obtained. Therefore, on the pattern tension specimen, about 50 nm silver film was deposited through an e-beam evaporation process.

To stretch the pattern, two 3-axis nano stages were combined with an optical microscope. (Figure 13, Figure 14) Several samples for tension were produced in a T-shape so that it could be pulled with a gripper. (Figure 21)

In general, if the patterns are stretched in one direction, it contracts in a perpendicular direction to it. However, the negative Poisson's ratio of the auxetic patterns used in this experiment complements this so that the patterns can be enlarged in all directions so that the pattern size can be maximized with a small tensile distance. In addition, it has excellent stability in tension. Therefore, it is very suitable for tension.

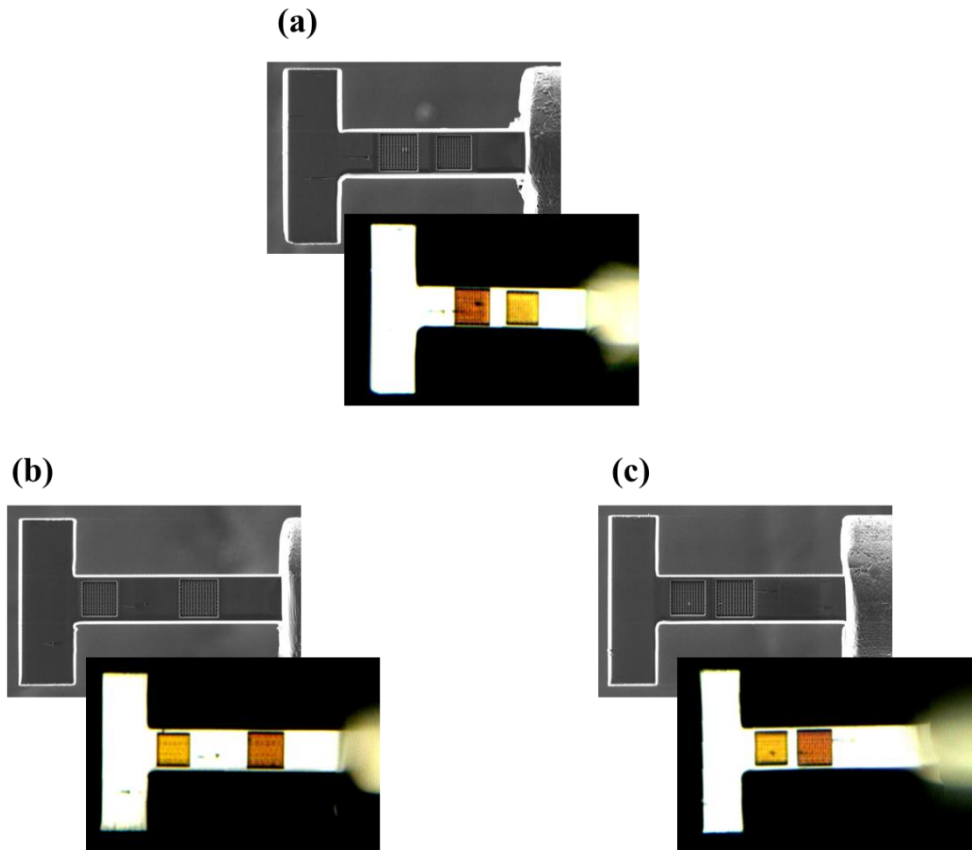

Figure 21. T-shape pattern samples for tension

5.1. Reflectance change of pattern under tension loading

This section shows the spectrum and color change when different size patterns are stretched. Figure 22 shows the results when the metamaterials in Figure 21 were tensioned. Based on the yellow pattern of the sample (pattern size : 500 nm × 810 nm), the maximum absorption occurred at 439 nm wavelength before stretching, but the absorption peak appeared at 500 nm after stretching. This could also be confirmed by optical microscope measurements. The yellowish color gradually changed to orange. In order to prove that the absorption peak is shifted according to the size change, the size change of the auxetic patterns was confirmed through microscopic image analysis. As a result, it was verified that one auxetic pattern was increased by about 55 nm and was similar to the degree of the peak position shift.

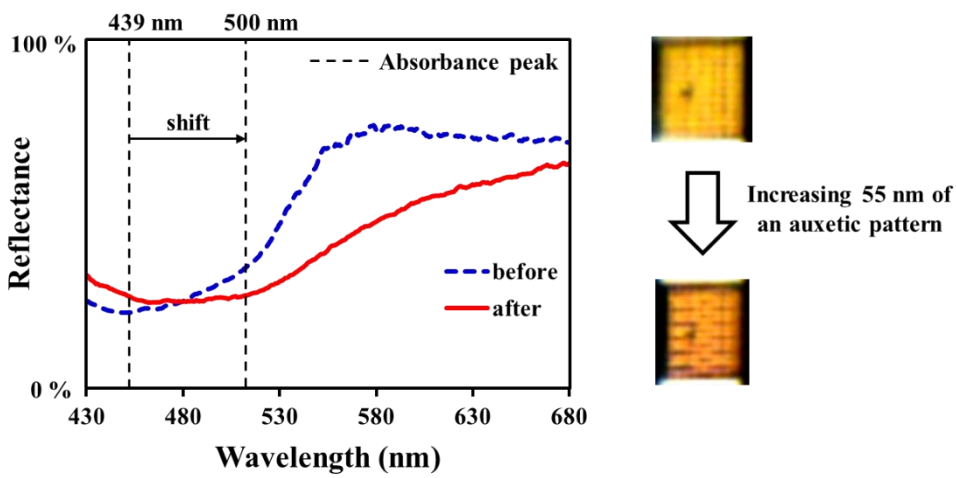

Figure 22. Color and spectrum change of 500 nm × 810 nm pattern under tension loading

Second, the same experiment was conducted for a pattern having a size of 605 nm × 990 nm. The results are shown in Figure 23. The color that showed a slight magenta tendency before tension had a more blue color after the tension. Spectrum measurements confirm this observation. The maximum absorption occurred before and after tensile at 564 nm and 595 nm respectively.

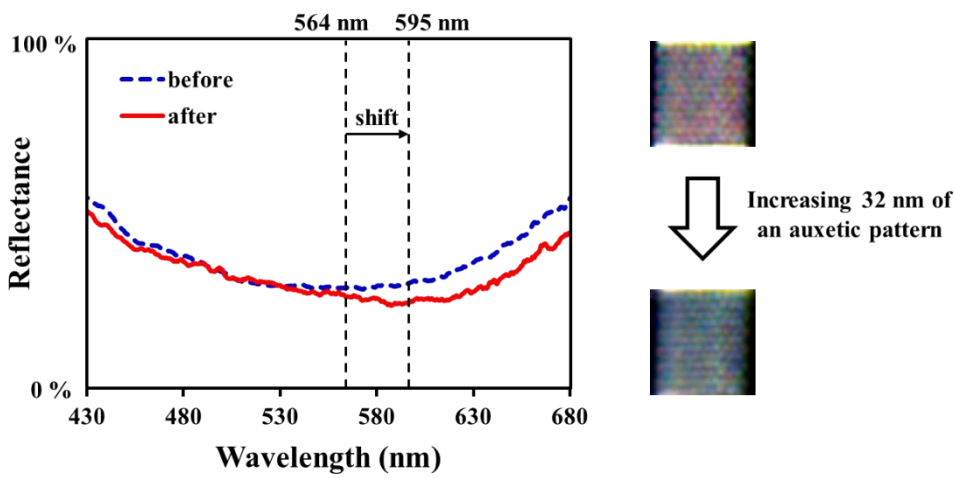

Figure 23. Color and spectrum change of 605 nm × 990 nm pattern under tension loading

The final tensile experiment was conducted in the same method for a pattern having a size of 560 nm × 915 nm. The results are shown in Figure 24. Initially, absorption was highest at 524 nm, but it shifted to 547 nm after stretching. As the overall tensile length was not large, the shift of the spectrum was small, so it was confirmed that the change in the reflected color was not obvious, but the color that was close to red was slightly pale.

Lastly, the pattern was restored to its original size by the shape memory effect, a characteristic of the SMA. As a result, it can be confirmed that the reflection spectrum almost completely returned to the spectrum before the deformation. Since the patterning area is small and the number of patterns is insufficient, the results of color change and spectral measurement are not very clear, but this tensile experiment proved the possibility for deformable plasmonic metamaterials.

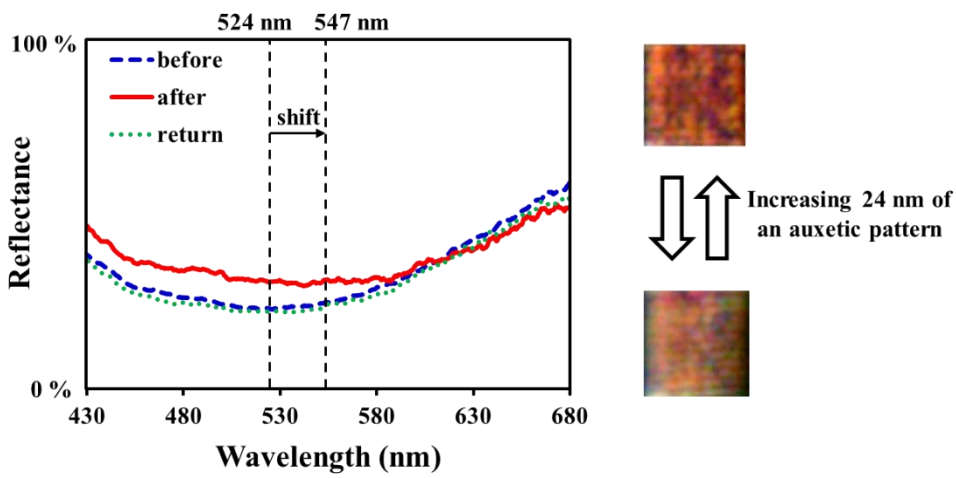

Figure 24. Color and spectrum change of 560 nm × 915 nm pattern under tension loading

5.2. Applications of deformable metamaterials

The plasmonic metamaterials that control the electromagnetic wave have been applied in various fields as explained in section 2.2, and have a huge potential that can be developed in the future. In particular, in this paper, deformable metamaterials using properties of SMA were developed, which not only are applicable to proposed applications but also make tunability. First, this tunability opens up the applicability to light modulators. The existing plasmonic metamaterial-based light modulator controlled light through a complicated pixel configuration and diode biasing method. [31] However, the metamaterials developed here can omit the complicated production process, which is time-consuming and costly, while enabling light control through simple a operation. Another accessible tunable metamaterial application is the color filter. Since our experiments showed that it can operate in the visible spectrum realm, it can be applied in the manner shown in Figure 25 through large-area patterning.

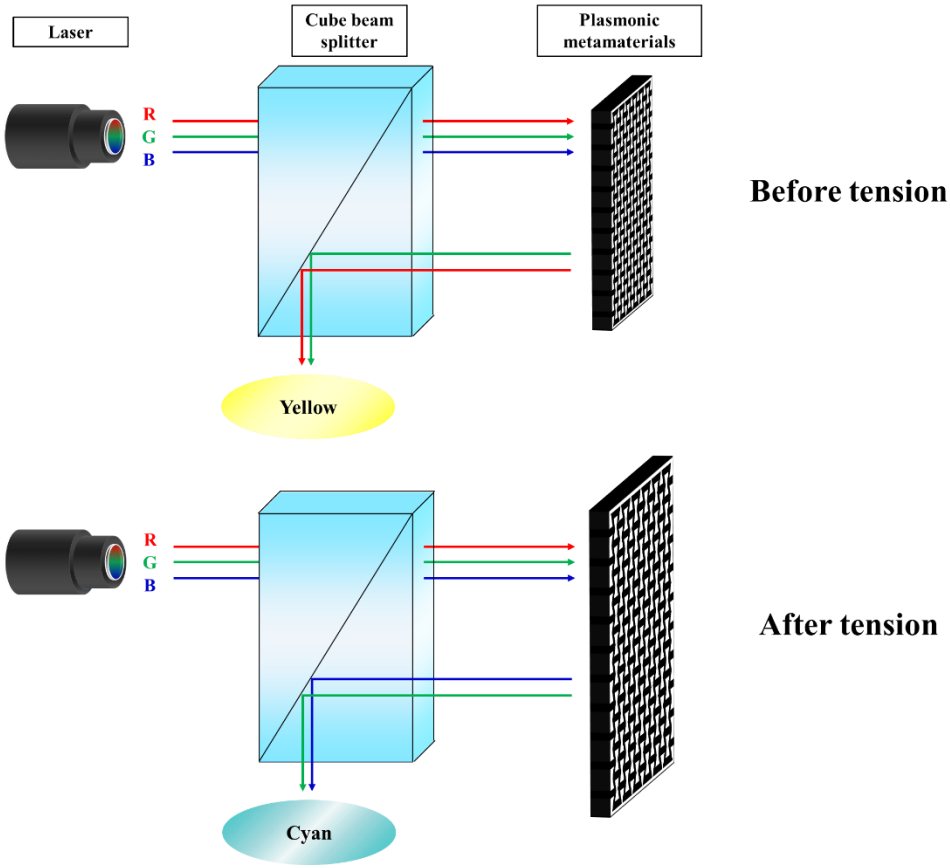

Figure 25. Application as a color filter of tunable auxetic plasmonic metamaterials

Chapter 6. Conclusions

Metamaterials are arrays composed of subwavelength nano elements and control electromagnetic waves based on their unique electric permittivity and magnetic permeability. Since they have special abilities that cannot be commonly found in nature, they have been steadily researched for use in a variety of applications since their inception. Nevertheless, currently developed plasmonic metamaterials have some problems to overcome. First, the manufacturing process is complicated, and the 3D structure cannot be manufactured due to process limitations. Second, most materials cannot be operated at a faster range than the infrared frequency. In addition, the plasmonic metamaterials developed to date have not escaped the stationary shape in that it uses metal. This is a very time-consuming and costly operation because it requires the structures of different sizes and shapes to operate at different wavelengths.

In this research, deformable plasmonic metamaterials were developed to overcome the hurdles encountered by these metamaterials. The LSPR effect was enhanced by coating gold and silver films through physical vapor deposition on auxetic nano patterns based on a shape memory alloy fabricated by using a focused ion beam. First, the reflectance was measured depending on the pattern size. When the gold film was deposited, the colors except for the blue area were confirmed, and when the silver film was deposited, all CMY colors were observed. And the change in reflectance was also confirmed when patterns were pulled. When the size of the pattern changed by up to 10%, the absorption peak shifted as much as it altered, and the reflection color changed from yellow to orange or from magenta to blue. Finally, the patterns were returned to its original size by the shape memory effect. This is the biggest difference from the previous research, so it is possible to control the light actively. Besides, it uses the localized surface plasmon resonance, so it has a

superiority that it is not angle sensitive.

The metamaterials developed in this research can be further improved. Despite the clear color observed by the eye, the actually measured spectrum was not as good as the simulated result. This is because the area of the patterning region is relatively small (7 μm × 7 μm or less) and reflectance is greatly influenced by external light. Also, the pattern thickness was not sufficiently thick, so that the tensile displacement could not be enough long. Nevertheless, since it proved the active movement of the absorption peak, it has great implications for the future aspects of the development of tunable metamaterials.

As discussed in the previous chapters, plasmonic metamaterials are being applied in most fields such as wave absorbers, light modulators, thermal emitters, color filters, biosensors where electromagnetic waves are being used. New relevant theories continue to be uncovered, and the scope of their application is gradually expanding. Although it is still insufficient in terms of cost, time, and stability to be applied as a practical device, metamaterials will overcome difficulties based on its potential to have a great impact on current nanotechnology.

References

[1] Zhang, F., Zhong, H., Chen, C., Wu, X. G., Hu, X., Huang, H., . & Dong, Y. (2015). Brightly luminescent and color-tunable colloidal CH3NH3PbX3 (X= Br, I, Cl) quantum dots: potential alternatives for display technology. *ACS nano*, *9*(4), 4533-4542.

[2] Barnes, W. L., Dereux, A., & Ebbesen, T. W. (2003). Surface plasmon subwavelength optics. *nature*, *424*(6950), 824-830.

[3] Lochbihler, H. (2009). Colored images generated by metallic sub-wavelength gratings. *Optics express*, *17*(14), 12189-12196.

[4] Diest, K., Dionne, J. A., Spain, M., & Atwater, H. A. (2009). Tunable color filters based on metal− insulator− metal resonators. *Nano letters*, *9*(7), 2579-2583.

[5] Jensen, T. R., Malinsky, M. D., Haynes, C. L., & Van Duyne, R. P. (2000). Nanosphere lithography: tunable localized surface plasmon resonance spectra of silver nanoparticles. *The Journal of Physical Chemistry B*, *104*(45), 10549-10556.

[6] Valente, J., Plum, E., Youngs, I. J., & Zheludev, N. I. (2016). Nano-and Micro-Auxetic Plasmonic Materials. *Advanced Materials*, *28*(26), 5176-5180.

[7] Takimoto, B., Nabika, H., & Murakoshi, K. (2009). Enhanced Emission from Photoactivated Silver Clusters Coupled with Localized Surface Plasmon Resonance. *The Journal of Physical Chemistry C*, *113*(27), 11751-11755.

[8] Smith, F. C., Scarpa, F., & Chambers, B. (2000). The electromagnetic properties of re-entrant dielectric honeycombs. *IEEE Microwave and Guided Wave Letters*, *10*(11), 451-453.

[9] Ding, S. Y., Yi, J., Li, J. F., Ren, B., Wu, D. Y., Panneerselvam, R., & Tian, Z. Q. (2016). Nanostructure-based plasmon-enhanced Raman spectroscopy for surface analysis of materials. *Nature Reviews Materials*, *1*(6), 1-16.

[10] Choi, B. H., Lee, H. H., Jin, S., Chun, S., & Kim, S. H. (2007). Characterization of the optical properties of silver nanoparticle films. *Nanotechnology*, *18*(7), 075706.

[11] Amendola, V., Pilot, R., Frasconi, M., Maragò, O. M., & Iatì, M. A. (2017). Surface plasmon resonance in gold nanoparticles: a review. *Journal of Physics: Condensed Matter*, *29*(20), 203002.

[12] Tao, H., Kadlec, E. A., Strikwerda, A. C., Fan, K., Padilla, W. J., Averitt, R. D., ... & Zhang, X. (2011). Microwave and terahertz wave sensing with metamaterials. *Optics express*, *19*(22), 21620-21626.

[13] Liu, N., Mesch, M., Weiss, T., Hentschel, M., & Giessen, H. (2010). Infrared perfect absorber and its application as plasmonic sensor. *Nano letters*, *10*(7), 2342-2348.

[14] Kumar, N., & Kumar, R. (2013). *Nanotechnology and Nanomaterials in the Treatment of Life-threatening Diseases*. William Andrew.

[15] Loos, M. (2014). *Carbon nanotube reinforced composites: CNT Polymer Science and Technology*. Elsevier.

[16] Landy, N. I., Sajuyigbe, S., Mock, J. J., Smith, D. R., & Padilla, W. J. (2008). Perfect metamaterial absorber. *Physical review letters*, *100*(20), 207402.

[17] Puscasu, I., & Schaich, W. L. (2008). Narrow-band, tunable infrared emission from arrays of microstrip patches. *Applied Physics Letters*, *92*(23), 233102.

[18] Seo, M., Lee, J., & Lee, M. (2017). Grating-coupled surface plasmon resonance on bulk stainless steel. *Optics express*, *25*(22), 26939-26949.

[19] Balaur, E., Sadatnajafi, C., Kou, S. S., Lin, J., & Abbey, B. (2016). Continuously tunable, polarization controlled, colour palette produced from nanoscale plasmonic pixels. *Scientific reports*, *6*, 28062.

[20] Genet, C., & Ebbesen, T. W. (2010). Light in tiny holes. In *Nanoscience And Technology: A Collection of Reviews from Nature Journals* (pp. 205-212).

[21] Kumar, K., Duan, H., Hegde, R. S., Koh, S. C., Wei, J. N., & Yang, J. K. (2012). Printing colour at the optical diffraction limit. *Nature nanotechnology*, *7*(9), 557.

[22] Kristensen, A., Yang, J. K., Bozhevolnyi, S. I., Link, S., Nordlander, P., Halas, N. J., & Mortensen, N. A. (2016). Plasmonic colour generation. *Nature Reviews Materials*, *2*(1), 1-14.

[23] Christiansen, A. B., Højlund-Nielsen, E., Clausen, J., Caringal, G. P., Mortensen, N. A., & Kristensen, A. (2013, September). Imprinted and injection-molded nano-structured optical surfaces. In *Nanostructured Thin Films VI* (Vol. 8818, p. 881803). International Society for Optics and Photonics.

[24] Cheng, F., Gao, J., Luk, T. S., & Yang, X. (2015). Structural color printing based on plasmonic metasurfaces of perfect light absorption. *Scientific reports*, *5*, 11045.

[25] Scarpa, F., & Tomlinson, G. (2000). On static and dynamic design criteria of sandwich plate structures with a negative Poisson's ratio core. *Applied Mechanics and Engineering, 5*(1), 207-222.

[26] Scarpa, F., & Tomlin, P. J. (2000). On the transverse shear modulus of negative Poisson’s ratio honeycomb structures. *Fatigue & Fracture of Engineering Materials & Structures, 23*(8), 717-720.

[27] Lee, H. T., Kim, M. S., Lee, G. Y., Kim, C. S., & Ahn, S. H. (2018). Shape memory alloy (sma)-based microscale actuators with 60% deformation rate and 1.6 kHz actuation speed. *Small, 14*(23), 1801023.

[28] Wan, H., Ohtaki, H., Kotosaka, S., & Hu, G. (2004). A study of negative Poisson's ratios in auxetic honeycombs based on a large deflection model. *European Journal of Mechanics-A/Solids, 23*(1), 95-106.

[29] Li, D. Y. (2000). Exploration of TiNi shape memory alloy for potential

application in a new area: tribological engineering. *Smart materials and structures, 9*(5), 717.

[30] Seo, J., Kim, Y. C., & Hu, J. W. (2015). Pilot study for investigating the cyclic behavior of slit damper systems with recentering shape memory alloy (SMA) bending bars used for seismic restrainers. *Applied Sciences, 5*(3), 187-208.

[31] Chan, W. L., Chen, H. T., Taylor, A. J., Brener, I., Cich, M. J., & Mittleman, D. M. (2009). A spatial light modulator for terahertz beams. *Applied Physics Letters*, *94*(21), 213511.

초록

형상기억합금 기반의 변형가능한 어그제틱 플라즈모닉 메타물질

임종혁

서울대학교 기계공학부 대학원

금속 나노구조체의 표면 플라즈몬 공명은 독특한 전자기 특성으로인해 지금까지 꾸준한 관심을 끌고있다. 특히, 입사광의 파장보다 작은 크기의 전도성 나노 입자, 나노 구조체로 빛이 입사할 때 발생하는 국소 표면 플라즈몬 공명은 파장 흡수기, 색 필터 및 센서 등에 적용돼 왔다. 이는 공진 주파수가 나노 구조체의 크기, 형상 또는 주위의 유전체 특성에 따라 달리 결정되기 때문이다. 그러나, 이전까지의 연구에서 개발된 플라즈모닉 물질들은 고정된 구조에서 벗어나지 못해 공진 주파수를 연속적으로 변경시킬 수 없다는 한계를 가지고 있다. 이 문제는 플라즈모닉 메타물질의 실제적 적용에 어려움을 주었다.

이번 연구에서는, 가시광 영역에서 공명 주파수를 이동시킬 수 있는 어그제틱 나노 패턴이 새겨진 플라즈모닉 메타물질이 개발되었다.

이 메타물질은 직경이 25 μm인 형상기억합금 와이어로 제작되어 패턴이 인장되고 열에 의해 복원될 수 있다. 이러한 메타물질을 제작을 위해서 집속이온 빔을 이용하여 1 μm 두께의 형상기억합금 필름을 제작했고, 뛰어난 기계적 물성을 가진 어그제틱 패턴을 그 위에 새겼다. 이후, 이온 코터 스퍼터링과 전자빔 증착방식을 사용하여 패턴위에 금과 은 나노입자를 증착하였다. 패턴의 인장을 위해서는 마이크로 그리퍼를 사용하였으며, 인장 후 355 nm 레이저를 이용하여 패턴을 원래의 형상으로 되돌릴 수 있었다. 패턴 크기의 변화에 따른 반사 효과를 확인하기 위해, 우리는 스펙트로미터를 이용한 흡수픽을 측정했을 뿐만 아니라, 광학현미경을 통해 직접 색을 확인했다. 또한, finite difference time domain (FDTD) 방식을 이용하여 동일한 모델에 대해 반사율을 계산했고 그 결과를 실험결과와 비교했다.

위와 같은 실험을 통해, 먼저 여러가지 패턴의 크기에 따라 다양한 색이 나타나는 것을 확인했다. 또한 패턴을 잡아당겨 그 크기를 약 10% 까지 늘렸을 때, 흡수픽이 이동하고 반사색이 변화하는 것을 확인했다. 최종적으로, 형상기억효과를 이용하여 원래의 패턴크기로 되돌림으로서 변형가능한 어그제틱 플라즈모닉 메타물질을 증명했다.

주요어: 표면 플라즈몬 공명, 형상기억합금, 어그제틱, 메타물질, 플라즈모닉

학번: 2018-26302